Spray Drying Technology Review

Richard Wisniewski[1]
NASA Ames Research Center, Moffett Field, CA 9403

This article reviews spray drying technology for possible space applications like processing of concentrated brines that are produced in evaporation/concentration equipment with a goal of maximum water recovery. Spray drying principles of convection, radiation and mixed convection-radiation are reviewed. Dryer designs and performance are reviewed. Subjects of system dynamics and controls are discussed. Adaptations of existing spray drying concepts to microgravity environment are suggested. Guidelines for design of the spray drying systems for space applications are proposed.

Nomenclature

I_N = Intensity Number; $I_N = f^2 * Am^4 /(C*Q)$; Am - amplitude, C - speed of sound , Q - flow rate, f – frequency.
Nu = Nusselt Number; $Nu = h*D_d /k$; h – heat transfer coefficient by convection; k – thermal conductivity of gas layer around droplet; D_d – droplet diameter.
Oh = Ohnesorge Number; $Oh = \mu_l/(D_d*\rho_l*T_s)^{0.5}$; μ_l - liquid dynamic viscosity; ρ_l - liquid density; T_s - surface tension.
Pr = Prandtl Number; $Pr = \nu/\alpha$; α – thermal diffusivity, ν – kinematic viscosity.
Re = Reynolds Number; $Re = D_d*u/\nu$; u – velocity.
Sc = Schmidt Number; $Sc = \nu/D$; D – diffusion coefficient.
Sh = Sherwood Number; $Sh = K_g * D_d /D$; K_g – mass transfer coefficient.
We = Weber Number; $We = \rho_g*u^2*D_d/T_s$; ρ_g - gas density, u - gas velocity.

I. Introduction

SPRAY drying, the process of turning liquid into solid product in one step, has found broad application in the food, pharmaceutical, chemical and nanotechnology industries. The spray drying process has been considered as a possible method for drying concentrated brines generated in the space life support system for water recovery. Other possible applications may involve production of nanomaterials (nanoparticles, nanocatalysts, nanodrugs), or fine particles and powders. The simple principle is employed by fine spraying a liquid into a hot gas stream, evaporating and drying the droplets in-flight and separating and collecting the solid particles from the gas stream. The process is very fast and product-gas contact is very short. Temperature of the gas decreases rapidly due to the intensive evaporative cooling while the droplet temperature remains low and thermally sensitive products can be processed. The droplets and particles movement follows the gas streamlines inside the dryer. The particle temperature increases during the drying and may reach the outlet gas temperature. Then the gas temperature is already significantly lowered due to the evaporative cooling and the product can be thermally safe. For example, thermally sensitive products like vaccines can be spray dried using air inlet temperature of 150 C [Roser, 2005]. The size of the produced particles, and the suspension flow and liquid atomization patterns may affect the design of the spray drying chamber. For larger particles the settling velocity of the particle needs to be taken into account, whereas the fine particles may follow the gas stream, thus the aerodynamic phenomena in the drying chamber can be critical.

The microgravity environment offers additional benefit of lack of significant settling velocity of the large droplets and particles. Thus the design of the drying chamber may depend on the desirable droplet size and particle drying time and their residence time inside the chamber. The droplets and particles may be maintained in suspension for a necessary time to complete the evaporation and drying steps. Industrial spray drying installations can be very large, but preliminary research is done in small laboratory systems. If results are promising, the next step of research

[1] Physical Scientist, SCB Branch, Mail Stop 239-15, Moffett Field, CA 94035.

and development is a scale-up step and is conducted in a pilot installation. The data obtained serve as basis for design of large scale spray drying system. In the case of possible space applications, the laboratory scale spray dryers may be close to the needed system scale, thus no pilot-scale tests may be required. The research done in a laboratory scale may be transferrable to future space bound systems. The gas velocities inside the laboratory spray drying systems are high thus there may be very little gravity effect until the solid particles reach the solid-gas separator. Particle separators like cyclones are affected by gravity in the solid discharge zone. Other separators, such as electrostatic precipitators, or membrane or cloth filters may be affected by gravity, but may operate satisfactorily in microgravity. For fine particles below 10 micrometers in size, the gravity effects are small since the settling velocity of such particles is slow. Often in the regulated industries, rechecking the operational parameters and product quality requires scaling-down the operation from the existing industrial systems back to a pilot system or even to a laboratory system level. Since the scale-up and scale-down are widely used approaches, small laboratory systems are easily available pieces of equipment and systems vendors possess databases for different products and drying conditions, thus are able to provide some expertise and assistance. They allow testing various spray drying conditions, droplet formation, heat delivery, particle separation methods, and concept of open or closed loop. There are commercial laboratory spray drying systems offered by the Swiss Company BUCHI, British company Keison, and Japanese companies Yamato Scientific and Fujisaki Electric. Further details of spray drying technology and systems can be found in the report by Wisniewski [2014]. In addition to dryers' review, it also covers topics of thermal radiation, particle separation, liquid atomization and vapor condensing.

II. Spray Drying Technology and Systems Review

A. Processed liquids

Convection spray dryers are used for production of powder products from a wide variety of liquids. Liquid properties relevant to spray drying are: solids content, density, surface tension and viscosity. High concentration of solutes in the liquid is desirable to increase dryer thermal efficiency. Liquid components should be thermally stable to withstand thermal treatment in the dryer. For example, the brines containing urine, may have a temperature limit to prevent urea decomposition and ammonia formation. Kontin et al. [2010] reported on investigation of drying of droplets of aqueous solution of urea. They demonstrated that if the solution and particles are kept below 400 K (127 C), thermal decomposition of urea may be avoided. Therefore, design of the spray drying conditions to process urea-containing brines may consider the droplet and particle temperature not exceeding 120 C. Brines with addition of surfactants may produce droplets of smaller size, different spray pattern and different drying characteristics due to surfactants located on the droplet surface. Increase in liquid viscosity results in increased droplet size [Spraying Systems Co. company literature]. Brine properties may change from batch to batch including concentration of solutes, viscosity and surface tension and spray drying process will be affected. The system design and controls, as well as choice of operational parameters should provide flexibility and robustness to be able to cover such variations in property.

B. Droplet generation

Industrial spray dryers employ a variety of liquid spraying devices. Droplet generation is often called liquid atomization. The large scale systems typically use rotating disk atomizers, or single fluid high pressure swirl nozzles. Smaller installation may use swirl nozzles or multiple-fluid spray nozzles, in which the droplet generation is caused by high velocity compressed gas jet. In the small, laboratory scale systems, typically multi-fluid nozzles and ultrasonic spray nozzles are used. Spray pattern and its interaction with drying air may determine uniformity of drying for droplets in different locations within the spray. The rotary disk atomizers and swirling nozzles with hollow cone spray pattern produce thin sheet of droplets that cross-interacts with the stream of drying air. Other spray patterns, such as solid cone, may produce a slower-drying spray core.

The spraying device manufacturers can provide data on the droplet generation performance, but in most cases the data are based on spraying water. Preliminary comparison may be conducted using such data, but experimental work is required to test the droplet-generating devices with processed liquids.

C. Droplet evaporation and drying

Droplet evaporation is a simple process and can be conducted in a free fall or using a moving carrier gas. Spray drying technology uses convective drying with hot air as a drying agent. Air contacts the spray and droplet evaporation and drying occur. Simultaneous heat and mass transfer take place, whereby heat is transferred from air to droplet by convection. Vapor is transported from the droplet to air by convection through the droplet boundary layer. If droplet and air velocities differ due to operation of the hot air distributor and droplet generator, there is also exchange of momentum between droplets and air. Droplets then follow the air stream and the relative air to droplet velocity can become small. Initially the droplet evaporation rate in the spray is nearly constant. The drying air temperature rapidly decreases. The droplet surface temperature is almost constant and may be represented by the wet bulb temperature. The partial water pressure at droplet surface is also almost constant during this period. Most water is removed during this period. At certain moisture content the droplet changes into wet particle and the process changes – moisture removal rate decreases, and temperature of particle surface increases. When particle becomes dry its temperature is close to the surrounding gas.

When droplets travel together with the air stream and the relative droplet to air velocity is small, then the heat transfer to the droplet may be approximated by using the Nusselt Number: $Nu = h*D_d/k = 2$; where: h – heat transfer coefficient by convection; k – thermal conductivity of gas layer around droplet; D_d – droplet diameter. The mass transfer can be represented by the Sherwood Number: $Sh = K_g * D_d/D = 2$; where: K_g – mass transfer coefficient; D – diffusion coefficient; D_d – droplet diameter.

Droplet evaporation rate increases if the relative droplet-to-gas velocity increases due to the convection effects in the boundary layer around the droplet. Frequently used equations for Nusselt and Sherwood Numbers involve Reynolds, Prandtl and Schmidt Numbers [Ranz, Marshall, 1952; Masters, 1991].

Reynolds Number $Re = D_d*u/\nu$; Prandtl Number $Pr = \nu/\alpha$; Schmidt Number $Sc = \nu/D$

Heat transfer $Nu = 2 + 0.6* Re^{0.5} * Pr^{0.33}$

Mass transfer $Sh = 2 + 0.6 * Re^{0.5} * Sc^{0.33}$

Where: D_d – droplet diameter; D – mass diffusivity; α – thermal diffusivity; ν – kinematic viscosity; u – velocity. Corrections may be applied to the above equations for droplets larger than 100 micrometers.

An example of droplet evaporation in a free fall:

Assume water droplet falls in dry air at temperature 30 C at pressure 0.1 MPa. Droplets diameter = 0.1 mm. Droplet diameter decreases until droplet completely evaporates. Under Stokes conditions, the droplet fall velocity is

$u= \rho^2*(\rho w - \rho) *g/(18* \mu)$;

where: ρ – gas density; ρw – water density; μ – gas viscosity; g – gravitational constant. Without internal circulation in the droplet, the droplet steady fall velocity is close to 0.3 m/s and Reynolds number for droplet is about 1.93. As droplet evaporates and its diameter decreases, the Reynolds number decreases. At Re<2, droplet falls under laminar flow conditions. Mass transfer coefficient for evaporation can be estimated using the Sherwood Number: $Sh=2+0.6* Re^{0.5}*Sc^{0.33}$; $Sh=k *D_d *R* T / D$; hence

$$k=D* (2+0.6* Re^{0.5}*Sc^{0.33})/(D_d *R* T) \qquad (1)$$

Water evaporation rate:

$$W=k*(p_s-p)* M* F = \pi*D* p_s*M *D_d * (2+0.6 *Re^{0.5}*Sc^{0.33})/(R* T) \qquad (2)$$

And from mass balance: $-(dm/dt) = -(\pi\rho D_d^2/6) D_d\ d/dt$.

Using droplet free fall velocity, $Re=D_d^3(\rho_w - \rho)\rho_g/18\mu^2$

the droplet free fall time until complete evaporation is about 4.6 sec. Droplet free fall height until complete evaporation is about 0.646 m. Droplets of 0.1 mm are in the droplet size range produced in the large spray dryer liquid atomization systems. Smaller droplets may evaporate faster and their free fall velocity is lower. Practical solution droplet data on the free fall, evaporation and drying in air were provided by Grisso et al. [2014], [Table1].

Table 1. An example of evaporation of pesticide solution droplets in a free fall [Grisso et al., 2014].

Droplet diameter (μm)	Terminal velocity (m/sec)	Final drop diameter (μm)	Time to evaporate (sec)
20	0.012	7	0.3
50	0.075	17	1.8
100	0.273	33	7.0
150	0.510	50	16
200	0.720	67	29

Liquid: Pesticide solution (3.75% w/w); air parameters: 33 C, 36% RH.

The 100 micrometer droplet drying with solids would take 7 seconds, and droplet would fall 1.91 m during this time. Fine droplets of size close to 20 micrometers or smaller can be easily dried in the small spray dryers. They follow the air flow pattern in the dryer and their residence time can be related to the air residence time. Manufacturing of nanoparticles and particles used for inhaled drugs required production of particles in size from submicron to a few micrometers. Very fine droplets can dry rapidly before they reach the dryer wall allowing usage of more compact dryers. Droplet drying in spray dryers occurs differently from the single droplet drying due to the droplets interaction, varying exposure of droplets in the spray to the drying air, changing droplet velocities, and changing properties of the drying air, including its temperature and humidity. The solution droplet drying involves multiple stages: droplet evaporation (1st stage of drying), formation of wet particle and drying of wet particle (2nd stage of drying) and final drying of moisture residue [Mezhericher, 2011]. During this process, the droplet temperature in the first stage is approximately constant, the wet particle temperature increases in the second stage as the moisture level in particle decreases, and the particle reaches temperature that is close to the surrounding gas temperature during the final stage of drying of the moisture residue. Particle breakage may occur during the second stage. The drying gas temperature rapidly decreases during the first stage due to evaporative cooling, modest decrease in gas temperature occurs during the second stage, and the gas temperature levels off during the final stage of moisture removal.

Dryers that combine radiation and convection heat delivery to droplets pose a challenge to heat and mass transfer analysis. Miliauskas and Sabanas [2005] reviewed computational approaches to water droplet evaporation, including heat transfer by convection, conduction and radiation. Droplet surface temperatures were calculated depending on heat transfer and on ambient conditions, such as air humidity. Combined effects of convection, conduction and radiation were discussed. Tseng and Viskanta [2006] investigated the effect of droplet evaporation on fire suppression and enhancement of droplet evaporation by radiation absorption. The finer the droplets are the higher their radiation attenuation. Water droplets were considered as semi-transparent to radiation. Droplet diameter decreases in time with convection and convection with radiation were compared. Droplet evaporation and size decrease was enhanced by the presence of radiation. The authors compared results to the earlier work by Miliauskas – their model showed larger effect of radiation. The droplet surface temperature was comparable to Miliauskas' data as well as the equilibrium evaporation rate.

Godoy and DesJardin [2009] developed a computational model of water polydisperse spray evaporation considering radiative attenuation in a 1D domain. Evaporation rates of droplets of different sizes were evaluated. Radiating wall temperatures of 1,200 K and 1,000 K were compared. Despite strong radiation absorption by water at 1,000 K (wavelength 2.9 micrometers), the evaporation rate was higher at 1,200 K due to higher radiation flux. Miliauskas et al. [2012] reviewed modeling of combined heat and mass transfer of water droplets in thermal technology equipment. Water droplet evaporation process was numerically modeled under various heat and mass transfer conditions. Modeling was performed using the combined analytical – numerical method to investigate heat and mass transfer in the two-phase droplets-gas flow system. The effects of forced liquid circulation were represented by the effective coefficient of thermal conductivity. The rate of droplet evaporation and the intensity of convective heating were calculated. Miliauskas et al. [2013] investigated initial water temperature effects on evaporation of droplet using computational model. They concluded that sprayed water temperature has a significant influence on droplets unsteady evaporation process. Initial temperatures of investigated droplets were below the evaporation temperature (293 K) and above evaporation temperature (363 K). Radiation absorbed by droplets may accelerate their heating if initial water temperature is lower than equilibrium evaporation temperature, and may slow the droplet cooling process if the initial water temperature is higher than equilibrium evaporation temperature.

Using water droplets may serve as illustration for possible methodology. However, the processed liquid droplets may behave differently from pure water droplets and one has to check whether adaptation of successful methods used for water droplets could be feasible. The processed liquid properties have to be well known. Such approach might provide some estimates, yet experimental work has to be conducted with the liquid of interest, including droplet heating, evaporation and drying while taking under consideration droplet size change and solid particle formation.

D. Spray drying process

In industrial applications, spray dryers are often used for large quantity production (examples: milk powder or detergents) and the sizes of drying chambers could be enormous (comparable to the size of multiple story buildings). The dimensions are related to dryer capacity and to droplet drying time. Depending on used spray devices, droplet size could reach several hundred micrometers with long drying time. Such droplets settle fast and may require a long flight time to dry, thus affecting the size of the drying chamber. Very fine particles are not preferred since their small size may adversely affect the particle separator performance and make the powder handling more difficult. The particle separators are typically cyclones followed by self-cleaning bag filters.

In many advanced applications, quantities processed are often relatively low and small particles may be required. Progress in spraying device design made it possible to obtain very small droplets with a narrow droplet size distribution. Such droplets dry faster and in more uniform time. However, resulting fine particles may still be difficult to separate at micron and sub-micron sizes.

Often the droplet evaporation research involves drying of single droplets [Fu et al., 2012]. The droplets can be suspended on a fiber or needle. Recent development has been use of acoustic levitators that can maintain a droplet freely suspended and subject to study different evaporating conditions. The microgravity may not only permit the studies on individual droplet evaporation without droplet settling, but also can provide conditions for multiple droplet evaporation as it may occur in the spray. In the terrestrial conditions one may employ very fine droplets with very low settling rates. Such fine droplets dry rapidly, thus requiring a small size of the drying chamber. The issues that may need to be addressed can be uniform heat delivery to all the droplets and efficient separation of the produced particles.

The droplet size and the resulting particle size have to be selected regarding two main criteria: the drying time and practically achievable particle separation efficiency. The finer droplets dry rapidly but the resulting small particles may be more difficult to separate, collect and handle. The required droplet size and liquid feed delivery capacity may dictate the choice of liquid atomizer design.

In general, finer droplets require shorter droplet residence time and therefore the drying chamber dimensions can be smaller. The separator could be a two stage type using, for example, a self-unloading/self-cleaning electrostatic precipitator followed by a self-cleaning filter. Development work is required for such designs.

Instead of an electrostatic precipitator, a bag filter with one or two walls can be used for particle separation. The bag filter may be of a disposable design. The first bag wall may capture coarse particles and the second wall fine particles down to a sub-micrometer size. Bag filters have a good operational track record in many industrial applications, for example, gas filtration at high temperatures for cleaning gases from boilers or incinerators. The emissions of particulate matter vary, ranging from < 1 mg/m^3 to over 1,300 mg/m^3. Particle sizes are in the range 1-80 micrometers. The pressure drop across the bag wall increases gradually as particles are captured. In one example, the pressure drop increased from an initial 14 mm water gauge at zero dust load to 36 mm water gauge at the load of 1,300 g/m^2 with a filtration velocity 0.5 m/sec [Morcos, 1996]. Bags are made of dense fabrics that should have good chemical and temperature resistance. Bag fabrics can handle temperatures close to 500 C. An example of the bag: The filter bags made of polyimide (PI) and polyphenylensulfide (PPS) needle felt. The felt has a specific weight of 624g/m^3 and 73.5 l/dm^{2}min permeability corresponding to 200 Pa pressure drop [Saleem, Krammer, 2007].

E. Drying air flow pattern

The drying air-spray interaction is the important part of spray dryer operation. The large industrial dryers can have variety of air flow patterns including co-current, counter-current and mixed flow pattern regarding the liquid spray direction. Most of the dryers are of the co-current air flow pattern and of the mixed flow pattern which involves a cross-flow combined with a co-current flow. The mixed flow pattern is used with rotary disk type liquid atomizers where the first air-spray contact may occur in a cross flow. The air entry into the drying chamber may use a straight or swirling flow pattern.

Uniform contact between the drying air and liquid spray is a part of good spray dryer design requirements. The small droplets trajectories may follow the air stream flow pattern. The current approach to spray dryer aerodynamic design is based on the past experience and on the computer modeling [Julkland, Golman, 2014] and on the computational fluid dynamics (CFD). Mezhericher et al. [2009] compared 2D and 3D CFD modeling of droplet drying in spray chambers. The authors suggested that the 2D model can be used for quick estimates for velocity, temperature and vapor mass fraction in the spray chamber. Mezhericher [2011] published a book on theoretical modeling of spray drying processes, including the drying kinetics and 2D and 3D CFD simulations. The topics covered are drying models of single droplet, heat and mass transfer of wet particles in the second drying stage, two-dimensional modeling of spray drying, three dimensional modeling of spray drying, effects of droplet-droplet interactions and particle-particle interactions, and predictions of air flow patterns using the k-epsilon and Reynolds stress turbulence models. The CFD approach may allow analyzing the air and droplets velocity distributions, air and droplet temperatures and progress of drying within the stream [Anandharamakrishnan, 2013; Mezhericher, 2012; Saleh, 2010]. The flow patterns and turbulence in the dryer may contribute to particle-wall contact [Shraiber et al., 1990]. Zaman and Bergstrom [2012] compared the turbulence models for particle-gas flows near the dryer walls. The CFD calculations may consider specifics of the near wall suspension flow including the wall surface roughness.

F. Small scale spray dryer systems

Possible space applications of spray drying technology may be limited to the small scale systems. The systems to be considered in the process of concept development and preliminary design may be selected from the commercial products used in laboratory experiments.

F.1. Convection-based systems

Industrial spray dryers are of convective type with hot air or inert gas used as a drying agent [Figure1].

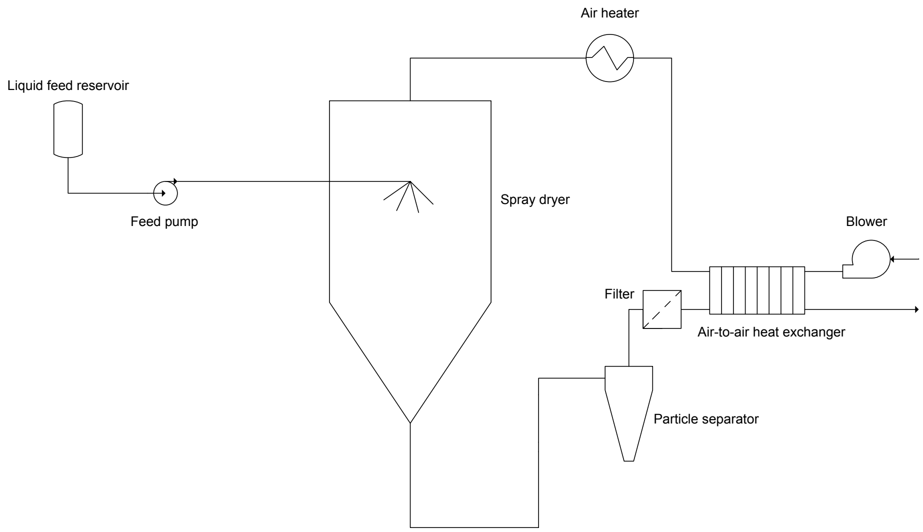

Figure 1. Spray dryer with ambient air as drying agent.

The convection-based spray dryers that are used in laboratory work may be considered for estimate of system performance and collection of preliminary experimental data before formulating concepts of a dryer and system design for space applications. Four commercial laboratory systems have been identified: B-90 Nano Spray Dryer and B-290 Mini Spray Dryer (by BUCHI, Switzerland), LabPlant SD-05/06 spray dryer (by Keison Intl, UK) and ADL311 spray dryer (by Yamato Scientific, Japan).

The B-90 dryer uses an ultrasonic spraying device and the B-290, SD-05/06 and ADL311 dryers use two-fluid spraying nozzles (the B-290 dryer can use an ultrasonic spraying nozzle). The B-290, SD-05/06 and ADL311 dryers use the cyclone particle separators and the B-90 uses an electrostatic precipitator separator. These main particle separators can be followed up by a filter separator.

The basic characteristics of these 4 systems are as follows [Table 2]:

Table 2. Specifications of laboratory scale commercial spray dryers.

System	B-90	B-290	SD-05/06	ADL311
Dryer image				
Water evaporation max. [mL/h]	200	1,000	1,500	1,300
Inlet air temperature max. [deg C]	120	220	250	220
Air flow max. [m^3/min]	0.16	0.58	1.17	0.7
Liquid feed flow max. [mL/min]			32	26
Air Heater [kW]*	1.4	2.3	3.0	2.8
Weight [kg]**	66	46	73	80
Dimensions** WxDxH [mm]	580x550x1,100	650x700x1,100	620x500x1,050	580x420x1,125
Power [kW]*	1.5	2.9	3.7	3.7

* power may depend on AC voltage used; ** designs not optimized regarding weight and dimensions

a) BUCHI spray dryers Nano B-90 and Mini B-290

a1) BUCHI Nano B-90 spray dryer

Estimate of performance of the B-90 Nano spray dryer at feed rate at 0.15 mL/min (9.0 mL/hr) [Table 3].

Table 3. BUCHI B-90 Nano spray dryer performance estimate.

Air in [C]	Evaporation [mL/min]	Air out [C]	RH out [%]
100	0.15	48.0	16.8
110	0.15	51.3	14.3
120	0.15	54.5	12.2

One may consider using higher air inlet temperatures due to the non-ideal contact between the spray and the drying gas. Considering practical experience, the above estimate may apply to practice in the range of inlet air temperature between 100 C and 120 C. For some products, a higher outlet air temperatures may be considered to decrease the outlet air relative humidity. Practical applications of this dryer involve small product quantities and low feed rates. An example of practical run: Salbutamol sulfate (an inhalation drug): Feed rate 10 g/h, gas inlet temperature 120 C, air outlet temperature 52-56 C.

a2) BUCHI Mini B-290 laboratory spray dryer

An example of the BUCHI Mini type dryer B-290 estimated performance in a closed loop using aqueous solution at low solids concentration: Configuration using two-fluid nozzle and atomizing gas; feed flow rate 6.00 mL/min (360 ml/hr; 8,640 ml/day); Heating air flow 580 L/min [Table 4].

Table 4. BUCHI B-290 Mini spray dryer performance estimate at feed rate 6 mL/min and air flow rate of 580 L/min.

Air in [C]	Evaporation [mL/min]	Air out [C]	RH out [%]
110	6.00	59.7	13.7
120	6.00	66.2	10.2
130	6.00	72.6	7.7
140	6.00	79.0	5.9
150	6.00	85.3	4.6
160	6.00	91.6	3.6
170	6.00	97.8	2.9

In this case, the drying air temperature should be above 110 C. Temperature in the range 120 C – 130 C can be feasible. To lower the air flow volume, one may decrease the drying air flow rate to 460 L/min [Table 5].

Table 5. BUCHI B-290 Mini spray dryer performance estimate at feed rate 6 mL/min and air flow rate of 460 L/min.

Air in [C]	Evaporation [mL/min]	Air out [C]	RH out [%]
120	6.00	56.8	18.6
130	6.00	62.6	14.3
140	6.00	68.3	11.0
150	6.00	74.0	8.7
160	6.00	79.7	6.9
170	6.00	85.3	5.5

In this case, the drying air temperature should be above 130 C. Air temperatures between 130 C and 160 C can be adequate. From the product thermal degradation point of view, one should not exceed 145 C. Further increase of inlet air temperature may be possible.
Configuration using ultrasonic spray nozzle: Feed flow rate 6 ml/min; Air flow 580 L/min; No atomizing air [Table 6].

Table 6. BUCHI B-290 Mini spray dryer performance estimate at feed rate 6 mL/min and maximum rated air flow rate of 580 L/min for ultrasonic spray nozzle option.

Air in [C]	Evaporation [mL/min]	Air out [C]	RH out [%]
110	6.00	57.5	15.1
120	6.00	63.7	11.3
130	6.00	69.9	8.6
140	6.00	76.0	6.6
150	6.00	82.1	5.2
160	6.00	88.1	4.1
170	6.00	94.1	3.3

In this case, the drying air temperature should be above 110 C with the reasonable temperature range between 115 C and 130 C.

A decrease in air flow rate may increase this temperature requirement: Air flow rate 460 L/min [Table 7].

Table 7. BUCHI B-290 Mini spray dryer performance estimate at feed rate 6 mL/min and air flow rate of 460 L/min for ultrasonic spray nozzle option.

Air in [C]	Evaporation [mL/min]	Air out [C]	RH out [%]
130	6.00	59.6	16.2
140	6.00	65.0	12.7
150	6.00	70.5	10.0
160	6.00	75.9	7.9
170	6.00	81.2	6.4

In this case, the practical drying air temperature should be above 135 C with reasonable temperature range between 145 C and 160 C. Air temperature levels near 140 C – 145 C may still be safe regarding urea decomposition due to the rapid droplet temperature drop in the drying chamber, but air temperature of 160 C may be too high. These are preliminary estimates – low values of RH may be considered.

Safe levels of inlet air temperatures are suggested; however, due to the relatively low outlet air temperatures, the inlet air temperatures may be increased. Practical safe temperature levels would need to be confirmed by experimentation. The air flow rate and temperature, and feed flow rate may be further optimized during practical runs, and productivity could be optimized without reaching levels of thermal product degradation, represented by urea.

Practical laboratory runs of the B-290 dryer often involve a relatively small temperature difference between inlet and outlet air, but the conditions may be dictated by product properties. The outlet air temperatures below 65 C are rarely reported. In other cases temperature differences similar to the industrial dryers data are used.

For example, drying the BSA-lactose for pulmonary delivery used air inlet temperature of 180 C and air outlet temperature of 70 C. This may be close to outlet gas 20% relative humidity and about 0.04 kg of water per kg dry air [Li, Saville, 2008]. Such high relative humidity may not be suitable for some products. Low outlet air temperatures were reported for some processes, but this involved lower air inlet temperature (for example, air inlet 95 C and air outlet 45 C for a similar BSA-lactose-surfactant mixture).

The above examples were estimated using low values of the outlet air relative humidity as it is expected in larger scale spray dryers.

Powder properties may also depend on the outlet air relative humidity. Air relative humidity may be related to moisture content in the powder. Another factor that may depend on air relative humidity is powder stickiness. This feature is important for the dryer operation – there must not be any powder sticking to the dryer walls and walls of outlet air ducting or particle separator. Even if the goal is water recovery and powder is a waste, the powder properties must allow reliable dryer operation including powder separation and removal. Powder stickiness needs to be determined experimentally. In general, one may consider increasing outlet air temperature and decreasing air relative humidity if there is any indication of a sticky powder. However, some powders may require reducing temperature below the glass transition point. Glass transition temperature may increase with lowering particle moisture content. A practical sticky zone may be at temperatures higher than the glass transition point. Additives are used to reduce the stickiness.

The additives may have high glass transition temperatures and after mixing them with the product that has low glass transiotion temperature, the resulting glass transition temperature may be higher thus increasing the sticking point temperature [Wang and Langrish, 2010]. These additives can be maltodextrin, gum, starch, or proteins. Woo at al. [2010] investigated amorphous particles collisions with the spray dryer wall and proposed a model that included impact velocity, particle size and particle rigidity.

Experimental runs using considered brines will be required to confirm acceptable dryer performance at the lowest possible air outlet temperature (highest possible outlet air relative humidity). These results may also depend on spraying pattern (type of spraying device used) and on the spray contact with the drying air, or on contact with the drying air combined with thermal radiation, since the air temperature drops very rapidly inside the drying chamber due to air-spray contact.

Computational fluid dynamics (CFD) analysis is often performed for large scale spray dryers, but less frequently for small dryers. Pin et al. [2014] performed CFD simulation analysis for the BUCHI B-290 spray dryer processing the *Piper betle* Linn extract using 3 turbulence models that can be considered in the CFD methodology. The droplet sizes were 36, 79, 123 and 166 micrometers and air inlet temperatures were 140 C and 160 C. The feed rates were 4, 9.5 and 15 mL/min. The authors reported that the k-epsilon turbulence model was the most suitable to predict flow behavior in the dryer.

b)Yamato Scientific spray dryer model ADL 311

Examples of spray drying using this system [Yamato Scientific data]: run with 10% of aqueous salt solution: Air inlet temperature 145 C; Air outlet temperature 85 C; Air flow rate 0.38 [m^3/min]; Liquid feed rate 5.3 [g/min]; run with 10% of oxidized titanium suspension: Air inlet temperature 150 C; Air outlet temperature 85 C; Air flow rate 0.42 [m^3/min]; Liquid feed rate 5.3 [g/min].

c) Keison spray dryers LabPlant SD-05 and LabPlant SD-06

Tan et al. [2010, 2011] investigated spray drying of whole milk powder and orange juice in the SD-05 dryer. For the whole milk drying the conditions were as follows: Inlet air temperature: 160 C, 175 C and 185 C; corresponding air outlet temperatures were 83.7 C, 91.8 C, 93.8 C, corresponding outlet air relative humidities were 13.1%, 9.7% and 9.6%. Liquid feed flow rate was 600 mL/hr. For the orange juice drying, the process conditions were as follows: Inlet air temperatures 130 C, 140 C and 150 C; corresponding outlet air temperatures were 89 C, 91 C, 95 C; corresponding outlet air humidities were 7.3%, 7.0%, and 6.5%. The feed flow rate was 360 mL/hr. In addition, the authors studied the dryer dynamics that is discussed in the later section of this paper. Since there are no data available for brines in this type and scale spray dryer, these data can be considered an example of products, which can be sensitive to temperature regarding degradation, as well as become sticky. Issue of stickiness has been known as a problem in spray drying of such products as fruit juices or carbohydrates. Brines may exhibit both problems of thermal degradation and stickiness depending on their composition.

d) Fujisaki Electric spray dryer MDL-015MGC

A similar laboratory spray dryer is made by Fujisaki Electric [Figure 2].

Figure 2. Fujisaki Electric MDL-015MGC laboratory spray dryer.

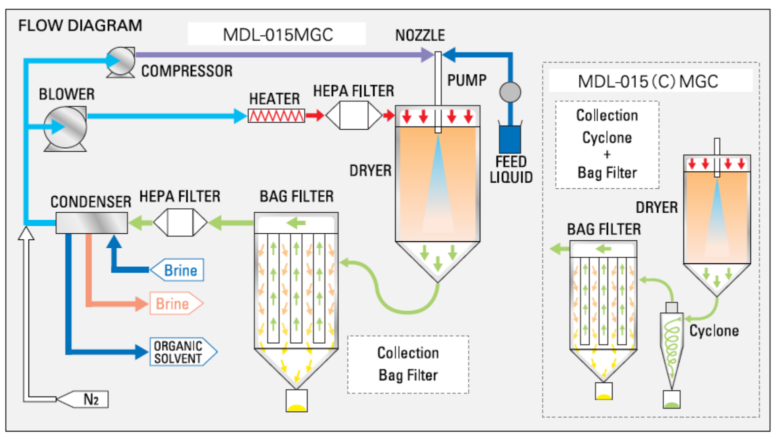

Figure 3. System schematic for laboratory spray dryer using multi-fluid spray nozzle with integrated compressor [Fujisaki Electric].

The evaporation rate is up to 1.3 kg/hr with electric heater rated 2 kW. The dryer uses a multi-fluid spray nozzle [Figure 8]. The atomizing gas pressure is 0.5 MPa (72.5 psi). The particles are collected in a bag filter placed in a separate housing. This dryer is of specific pharmaceutical design, therefore HEPA filters are used. The system is designed using stainless steel with highly polished surfaces. This system is designed for easy cleaning and disassembly/assembly in accordance with the pharmaceutical current Good Manufacturing Practices (cGMP) requirements. Its condenser can operate with coolant ("brine") that can cool organic solvents to -30 C. System is suitable for continuous operation. Figure 3 shows a closed system with solvent recovery that can be analogous to a water recovery system. An open system is also available. Particle separation is done in a bag filter, or in a combination of cyclone and bag filer.

F.1.1. Dryer design

Design process of the convection spray dryer may start with establishing air inlet temperature that provides safe treatment of processed liquid and dried product. Air temperature decreases rapidly after first contact with the spray, therefore the inlet air temperature might be higher than the product safe temperature determined in an oven test. The dryer outlet temperature may be estimated, yet experimentation is required to confirm this value. The amount of drying air is estimated based on the flow rate of processed liquid product. The drying chamber geometry may be estimated following the practical experience from existing dryer designs. The chamber geometry may depend on configuration of the drying air inlet, the air flow rate and temperature, and on the liquid atomizer design and performance. Experiments using a small laboratory dryer will be required. Possible chamber geometries may be studied using computational fluid dynamics.

The liquid atomizing device should be able to deliver droplets of certain mean diameter with narrow size distribution. Spray pattern and spray velocity may affect drying chamber design. Atomization device should be able to operate within a certain range of flow rate, as the flow rate adjustments may be used to control the process. The liquid delivery system that feeds the atomizer should have a short response time and work in a stable fashion during transitions in a flow rate.

F.2. Radiation and radiation/convection reactors and dryers

F.2.1. Radiation-based apparatus

A vertical column with a spraying nozzle at the top and thermally radiating walls can be a representation of radiation spray dryer. There may be no significant forced air flow and the dryer may operate in similar way as a prilling tower, e.g. droplets are formed at the top and they dry in free fall. Energy delivery is by radiation. Since there is no significant air flow, the dried particles are collected at the bottom. Droplet formation may induce certain droplet velocity that can be high using the high pressure and two-fluid spraying nozzles and usually is low in ultrasonic spraying device.

Radiation heat input is converted to latent heat of evaporation of droplets and dried particles. Vapor that forms can be condensed in a condensing heat exchanger, with release of latent heat of condensation. Due to lack of significant air flow, a possible place where the energy is recovered can be a condensing heat exchanger or an independent heat exchanger working together with condensing heat exchanger. Incoming liquid product can be pre-heated there by condensate. Introduction of some air flow into the column may aid in particle movement beyond the zone of spray device dynamic effects and also may facilitate particle collection in a filter or electrofilter. By introduction of air flow one may bring the dryer operation to a mixed radiation-convection mode of operation. In practical applications air moves through the dryer and its movement affects droplets velocity and may affect drying time due to convectional effects around the droplets.

Phenomena in the radiation-based apparatus may involve interaction of radiation with fine mist that is similar to fog. Radiation-fog interactions have been studied in atmospheric research. Saito [1956] studied transmission of infrared radiation through fog and a thin water layer. A water layer of thickness of 0.01 mm corresponded to 10 g/m^2 of fog. The difference between transmission through the water layer and corresponding fog was due to radiation scattering by fog droplets. The fog droplet sizes were 3.4, 4.1, 4.5 and 5.9 micrometers, e.g. within the range produced by vibrating disk ultrasonic fog generators. Kurnick et al. [1960] reported data on attenuation of infrared radiation by fog. The radiation wavelengths were in the range 1-11 micrometers. Optical density of fogs declined at the end of this range. The authors conducted measurements on natural atmospheric fogs. In a field of frost protection, fog density and droplet size may provide enough radiation absorption to prevent heat escape from the ground area. Smith and Knox [1987] reported the maximal radiation reduction (48%) occurred with droplets near 1 micrometer in diameter, thus inferring that the fog absorbed 48% of the initial radiation. Fog interaction with radiation involves scattering, absorption and re-emission of radiation.

F.2.2. Radiation/convection apparatus

There is abundant information available on convection spray dryers using hot gas, but limited information is available on spray drying using radiation heat transfer. Equipment nomenclature may not use terms “spray dryer” or “nebulizing dryer”. Therefore, search has been done to identify systems that produce fine particles using liquid atomization combined with thermal radiation. The classical thermal radiation literature [Siegel and Howell, 2001; Balaji, 2014] may not cover topics of radiation interaction with multiple droplets in complex reactor geometry. Related types of equipment have been tubular gas reactors, tubular “plug” reactors, laminar flow tubular reactors and aerosol flow reactors. These designs are typically based on a tubular furnace with reactor tube wall heated electrically. The wall transfers heat by thermal radiation and convection. In reactors operating at low pressures/vacuum, heat transfer occurs mostly thermal radiation.

Aerosol thermal reactions have been used for decades in manufacturing of fine particles [Pratsinis, 2011; Gurav et al., 1993]. In the simplest case, the wall temperature along the reactor is controlled to maintain constant temperature along the tube. There are inlet and outlet sections of the reactor, where temperature increases and decreases [Figure 4]. Central processing zone is sometimes called "flat zone" [Timedomain CVD, 2014]. Temperature control of the "flat zone" can provide control within less than 1 degree C accuracy. Temperature control is based on wall temperature and temperature stability can be maintained due to high thermal inertia of the furnace, thus adjusting wall temperature using the outlet gas temperature is impractical since the gas residence time in the reactor may not be comparable with the furnace dynamic response. Outlet gas temperature monitoring is used to maintain gas phase reaction consistency and resulting product quality. Measurement of gas temperature inside the tube is possible, but due to wall radiation effect, thermocouples need to have radiation shielding [White, King, 2009]. Such tubular heaters/reactors can have multiple heating zones that can be controlled independently thus providing pre-programmed wall temperature profile along the reactor.

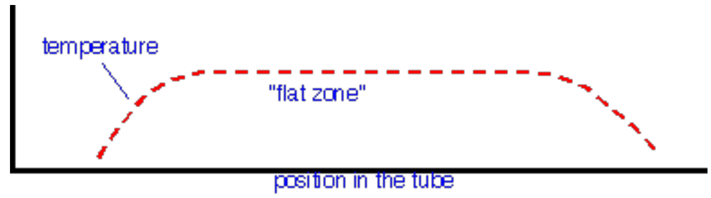

Figure 4. Temperature profile along tubular reactor.

F.2.3. Radiation/convection aerosol flow reactor

Thermal radiation based aerosol flow reactor schematics is shown in Figure 5. For reactor operating in a laminar flow regime of the carrier gas, velocity profile approaches a parabolic profile. If spraying device produces fine aerosol droplets and such aerosol is a fog-like, then the droplets may not significantly affect the carrier gas velocity profile. Diffusion dispersion that occurs in gas may not significantly affect the aerosol droplets. At high wall temperatures, heat will be delivered mostly by radiation, yet radiation would need to penetrate layers of droplets and dried particles to reach the tube center. Therefore, critical factors are the radiation absorption by droplets and particles and the transparency of layers of droplets and particles to thermal (infrared) radiation. The small droplets and particles would contribute to radiation scattering. Interaction between radiation and droplets results in attenuation of radiation energy by absorption and scattering. If the liquid contains any strongly radiation-absorbing substances, coloring substances or suspended particles, radiation effects upon cloud of droplets may differ from its effects on water droplets [Varghese, Gangamma, 2007]. Evaporation of pure water droplets might be used as a preliminary model, but experimental work is required using processed liquid due to droplet-radiation interaction and droplet evaporation differences between water and processed liquid. If the reactor wall cannot be heated to high temperature, then the part of thermal radiation energy transfer decreases, and the role of convection and conduction effects may increase.

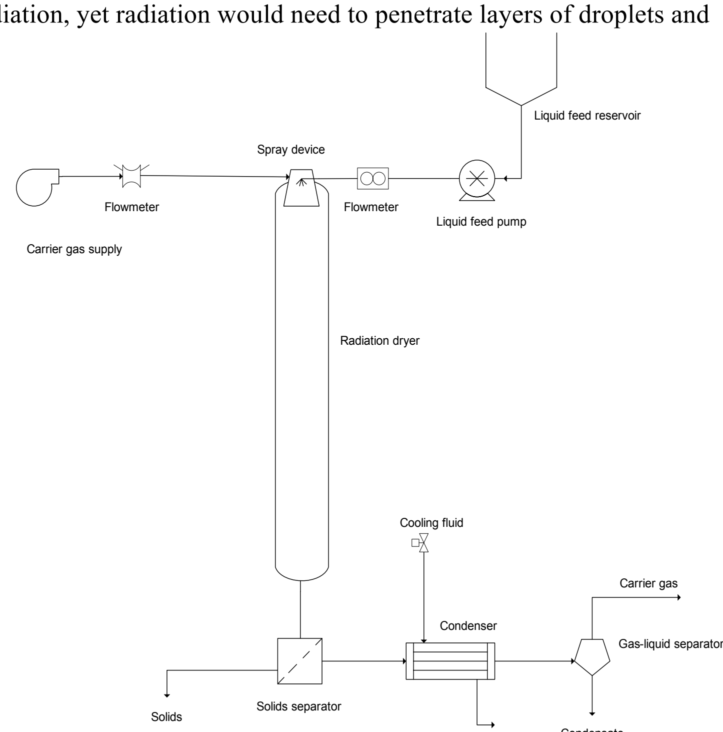

Figure 5. Diagram of aerosol flow reactor.

Under the laminar flow regime and in the absence of natural convection at the heated wall, heat transfer will be due to boundary layer heat transfer due to carrier gas flow. There will also be effects of natural convection, increasing heat transfer rate. Heat transfer rate under microgravity may be lower than under normal gravity due to the absence of natural convection. On another hand, the absence of natural convection at heated walls would allow maintaining less disturbed laminar flow approaching parabolic velocity profile. The energy radiated per unit of surface area is:

$$J = \varepsilon*\sigma*T^4 \quad (3)$$

Where: σ is the Stefan-Boltzman constant = $5.67*10^{-8}$ [$W/(m^2 * K^4)$], ε is surface emissivity, T is temperature [K].

If for example, the wall temperature is maintained at 120 C (393 K), then the thermal radiation heat transfer may be at about 811 W/m^2 using a stainless steel reactor wall with wall emissivity coefficient of about 0.6. The tubular reactor of 0.1 m diameter and 1.0 m length would have thermal radiation flux of about 255 W. This corresponds to capacity of about 400 mL/hr of water evaporated based on the latent heat of evaporation.

Other part of heat transfer is a laminar flow thermal conduction from tube wall to flowing medium. In a steady state and in laminar flow, heat transfer between the heated tube wall and flowing fluid may be determined using the Nusselt Number = 3.66. [Incropera and DeWitt, 1996; Abraham et al., 2009]. The Nusselt Number for pipe flow: $Nu = h*D_p/k$; where D_p – pipe diameter, h – heat transfer coefficient, k thermal conductivity of fluid. For 0.1 m diameter reactor, this would give a low heat transfer coefficient on the order of 1 [$W/K*m^2$]. In the reactor entry region the Nusselt Number values can be higher than 3.66.

Natural convection at the heated tube wall may alter the laminar flow heat transfer [Hausen, 1983]. With wall temperature decrease, the radiation part of heat transfer would decrease and heat transfer will involve conduction from wall to the boundary layer. The presence of droplets in the boundary layer makes heat and mass transfer more complicated due to factor of droplet evaporation [Terekhov, Pakhomov, 2014]. Terekhov and Pakhomov reported heat and mass transfer results for the case of mist flow over flat plate for laminar and turbulent boundary layers with the presence of droplets. Main stream of suspension had temperature 293 K and wall temperatures were in the range 323-473 K. Increase of tube diameter may increase radiation and conduction heat transfer area, but at the same time the Reynolds number increases thus to maintain laminar flow, fluid velocity in the tube may need to be decreased. Depending on the droplet diameter, carrier gas velocity has to be selected considering droplet settling velocity for systems operating under gravity.

In the flow reactors with laminar flow of gas, there may be not only the effect of natural convection at heated walls, but also effects of changing gas properties along the tube radius. As viscosity and density of gas change at the heated wall, the parabolic velocity profile of laminar flow gets disturbed. Even without the presence of aerosol, the parabolic velocity profile may get retarded at the wall and accelerated near the axis – shorter residence time near the axis would occur.

Practical reactor design should consider hydrodynamics of reactor inlet part prior to the heating section to stabilize flow of the carrier gas mixture with aerosol droplets. Thermal radiation heat transfer in circular tube also produces a focusing effect towards the tube centerline. This energy focusing effect will be distorted by the presence of droplets and particles within the reactor volume. For small diameter droplets, convection may dominate over radiation, and absorption of thermal radiation may have relatively small effect [Tseng, Viskanta, 2006]. Modeling analysis has been typically done for water droplets. For processed liquids results may not be possible to predict and experimental work is required to determine reactor performance conditions and its processing capacity. It may be important to have the processing capacity to vary broadly regarding the flow rate of aerosol, thus experimental work may begin at low feed rates that are gradually increased until reaching full reactor capacity. The reactor may require multiple heating zones located along the tube for better performance optimization.

A typical design of aerosol flow reactor can be an empty tube with heated walls, but there can be reactor designs with a central heater and tube walls insulated, or heated and insulated. The central heater surface area is smaller than the tube wall surface area, thus if only the central heater is applied, to deliver sufficient radiation energy, the heater surface temperature needs to be higher than in the case of reactor with the heated tube wall. Hwang and Lin [1992] reported on numerical modeling of a reactor with the central heater and insulated external wall. Due to computational difficulties, the authors applied a simplified model with multiple heat sinks representing the suspended droplets. Calculations with convection only and combined convection and radiation were performed. Droplet evaporation time was significantly shorter for the combined radiation and convection than for convection alone. Droplet diameter was 0.6 mm. The Nusselt Number reached 7.35 under steady state. Heater wall temperature was 871 C.

Tubular flow reactors have to be investigated for their dynamic responses to allow more realistic model building to be used for reactor performance simulation, design of control system and controls tuning. System identification techniques can be used for building dynamic model of the flow reactors [Ljung, 1999]. Experimenting with a particular real reactor design may lead to model development and implementation of model predictive control technique [Camacho and Bordons, 1995; Ocampo-Martinez, 2010]. Programmable logic controllers (PLC) and computers may be then used to implement the system control concept [Astrom, Wittenmark, 1999; Vodencarevich, 2010].

Aerosol-based processes have been used in manufacturing of nanomaterials [Buesser, Pratsinis, 2012] and in studies on aerosol particles formation [Ezell et al. 2014]. A related concept has been design of laminar aerosol flow tubes [Khalizov et al., 2006a,b]. Cooled laminar aerosol flow tubes have been used to study aerosol properties under conditions typical to troposphere and stratosphere. Practical reactor operation may be conducted with some temperature safety margin to maintain reactor wall temperature below product degradation temperature. However, to maximize radiation heat transfer, the wall temperature should be as high as practically possible. Analysis of fluid dynamics and heat transfer between the heated wall and carrier gas in the tubular reactor is the first step in modeling reactor performance. The presence of aerosol introduces significant complication to phenomena in the reactor and factors, such as aerosol droplets interactions with the carrier gas, droplets interactions with thermal radiation, and droplet-droplet interactions, have to be considered. Subject of droplet evaporation under thermal radiation in combustion applications has been extensively studied [Sazhin, 2006]; however, fuel droplet evaporation may not lead to formation of product particles as in spray drying. Dombrovsky and Bailis [2010] published a thorough review on interaction of radiation with dispersed systems, including the topic of droplet evaporation with energy delivery by thermal radiation. Processes with very high wall temperatures and under lowered pressure or under vacuum may operate in a mode with almost all energy delivered by thermal radiation. At lower temperatures, a mixed mode of radiation/convection heat transfer occurs. One of the processes performed in aerosol flow reactors has been spray pyrolysis [Reuge, Caussat, 2007]. This process has been used for producing many materials in a powder form. There are four main steps involved: spray formation; spray transport in air stream (droplet evaporation – precipitation may occur in droplets); thermolysis of precipitated particles; internal particle sintering. Particles are then separated from air stream. Spray pyrolysis may be conducted in high or moderate temperatures. Moderate temperatures produce uniform particles, while high temperature processes often produce hollow particles with hard shell.

F.2.4. Examples of fine particles production using aerosol flow reactors

There are numerous reports on fine particles and nanoparticles production utilizing systems carrier gas laminar flow with suspended fine droplets. Processing is conducted in tubular reactors with heated walls.

a) An example of nanoparticle-producing system [Okuyama, 2003]: fine droplets were generated in an atomizer and carried by the gas stream into a multi-zone furnace with 7 independently controlled heating zones. Furnace temperatures were set between 500 C and 1,700 C leading to pyrolysis of particles. The carrier gas flow rate was adjusted to provide a few seconds particle residence time in the furnace. There were no issues of thermal decomposition of processed materials. Flow of a carrier gas was downwards, e.g. opposite to natural convection effect at heated walls.

b) An example of laboratory setup for spray drying of dextrin that used radiation heat transfer with a possibility of thermal decomposition [Luz, 2007]: particle separation was done by filtration and condensation occurred in a flask cooled by water. Ultrasonic atomizer frequency was 1.66 MHz - able to produce fine droplets. Drying chamber was a two-zone furnace. Inlet and outlet temperatures were 280 C and 275 C. Operation was conducted below dextrin degradation temperature (may occur between 295 C and 300 C). Particle size was between 0.2 and 2.6 micrometer. Mean diameter determined by laser light scattering was 1.7 micrometer. Dextrin is a frequent additive in spray drying to reduce or eliminate particle stickiness and can be used for spray dried foods. About 60% of atomized feed was collected on filter membrane (rated 0.2 micrometer) in a powder form. There was no mention whether losses were in the drying chamber or following duct.

c) An example of radiation droplet evaporation reactor was the system used to produce amino acids nanoparticles [Lahde, 2008]. In this case, atomizer produced fine droplets with size 300 nm, far below droplet sizes occurring in commercial spray drying. A specialized nanodroplet generator was used. The reactor was a stainless steel tube placed in a furnace. Carrier gas flow was adjustable and droplet residence times were in the range of 9 to 11.1 sec. Experimental temperatures were 110 C, 150 C and 200 C. There was no condensing heat exchanger – exiting particles were cooled by injection of cool nitrogen gas through a porous tube. At 110 C, particles formed by droplet drying. At 150 C, the amino acid partially vaporized with residues remaining in particles – this may represent decomposition. Therefore, conditions could be related to drying of urea solution and its potential decomposition issue.

d) An example of pyrolysis of aqueous silver nitrate to produce nanoparticles was reported by Pingali [2005]. A furnace was used with a metal tube insert. Processing chamber was maintained at 650 C. Argon carrier gas was used to avoid oxidation. Carrier gas flow direction was opposite to natural convection effect. Mitrakos et al. [2008] reported CFD simulation of the tube furnace reactor for synthesis of silver nanoparticles. Plug flow (1D) and multidimensional CFD models were compared. The authors concluded that plug flow 1D model may provide sufficient modeling accuracy.

e) An example of pyrolysis in aerosol reactor under low pressure was reported by Delendik et al. [2012]. Their process was conducted at the pressure range 20-60 Torr. Rapid evaporation of droplets was observed. High velocity gas jet liquid atomizer produced droplets with size of 10 micrometers. These examples provide some insight into radiation-based droplet evaporation, drying and processing.

Industrial thermochemical processes often involve high temperature heterogeneous systems, in which reacting gas-particle mixtures are exposed to intense thermal radiation [Ebner, Lipinski, 2011]. Their thermophysical properties change during the process due to temperature and composition changes, and this may affect heat and mass transfer and chemical reaction rates. Ebner and Lipinski numerically analyzed the effect of radiative heating of a large semi-transparent particle undergoing heterogeneous thermochemical decomposition. They developed an unsteady numerical model coupling radiative-conductive-convective heat transfer and mass transfer to chemical kinetics. Thermal decomposition of $CaCO_3$ was selected as the model chemical reaction. Direct irradiation and internal radiative transfer in the particle were highly favorable for particle heating and decomposition reaction, substantially decreasing the total reaction. Without radiation, heat transfer in the particle is limited by the rate of convection at the particle surface and conduction inside the particle. The latter decreases with increasing particle porosity. External radiation was predominantly absorbed in vicinity of particle surface. Work was related to operation of high temperature solar thermochemical reactors.

The aerosol flow reactors have been mostly investigated empirically, with a relatively few reports on more thorough analysis, including use of computational fluid dynamics. White and King [2009] reported experimental and simulation (CFD) analysis results using a horizontal tubular reactor used to produce carbon nanotubes. While this concept has not attracted much attention in the traditional spray drying community, reported successful nanoparticle laboratory production may attract more interest in particle production in such reactors. The examples are of small scale and such scale might be compatible with future space applications.

F.2.5. The aerosol drying apparatus at NASA Ames Research Center

The aerosol drying apparatus at NASA Ames Research Center has been constructed by Umpqua Research Company as an SBIR Project and later modified in-house [Figures 6 and 7]. At the bottom of this apparatus, there is a vibrating disk liquid atomizer using multiple disks. The dryer column has a central rod heater and locally heated walls. An electrostatic particle separator is located at the top. Its operating voltage is 20 kV. Vapor is condensed in a vertical shell and tube condensing heat exchanger. The vibrating disk atomizer generates mist with droplet size around 5 micrometers at the fixed rate of 180-200 mL/hr. The carrier air flow rate is controlled and adjustable. The temperature is controlled by adjusting power to the central rod heater (rated 1 kW) and to the band heaters on the tube wall. There are several sheet and band heaters heating the tube's external wall (total rating 779 W). Actual power use can be lower than these heater ratings. Drying chamber outlet air temperature is used as a control parameter. During operation heaters power settings remain constant. The mass of system components is 42.05

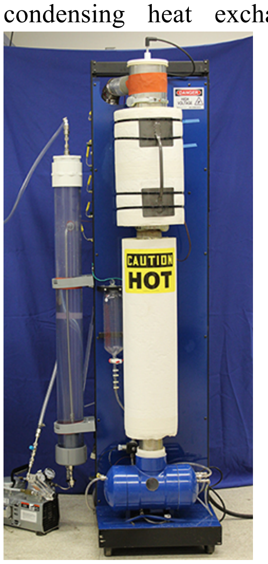

Figure 6. Aerosol drying apparatus [Umpqua Research Co.].

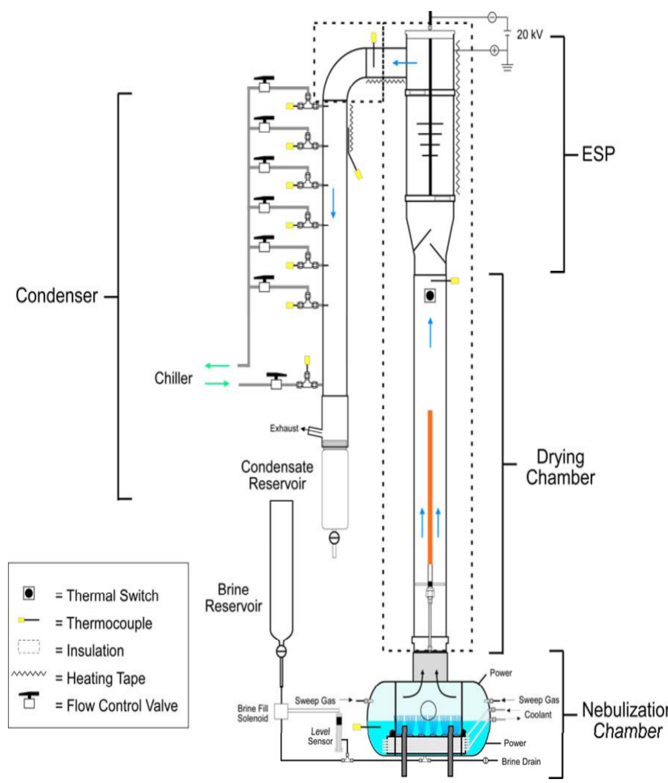

Figure 7. Aerosol drying apparatus - system schematics [Umpqua Research Co.].

kg without supporting structure and bubble column gas absorber scrubber. Height is 2,050 mm including supporting structure with casters. Components volume was estimated as 0.207 m^3 without the gas absorber (the gas absorber was designed in-house to additionally purify exit air; it is shown in Figure 6 on the left side of the reactor).
An example of early development run using brine: 484 mL (518 g) of brine was processed. Processing time was 160 minutes. Brine composition: 74.6 g of solids and 443.4 g of water. Amount of condensate collected was 420 mL. Mass of powder collected in electrostatic precipitator was 26.35 g with 2.35% moisture content [Umpqua Research Co. data]. Operational experience has shown that collected particles may fall from the tubular collection electrode into the radiation heater zone and thermal product degradation can occur.

F.2.6. Reactor/dryer design

Design process of a laminar flow aerosol reactor may begin with establishing the reactor wall surface temperature that provides safe treatment of liquid and dried product. Material of the tube, tube surface state and radiation emissivity coefficient of the tube are also established. Radiative heat input can be then estimated. Depending on the rate of processed liquid product, reactor heated surface area is estimated. Tube geometry selection involves not only the tube surface area, but also the diameter/length ratio and design of the inlet section to provide conditions of developed laminar flow.

If multiple heating zones are specified, then the heated surface area and reactor length should be extended since some of the zones may operate at lower temperatures established to obtain desirable product properties. For example, for early zone temperature may be higher due to evaporative cooling of the droplets, zone temperature may be lowered at the end of the reactor where the stream carries mostly dried particles. Flow rate of the carrier gas should be established to provide for flow rate adjustments while maintaining laminar flow within the range of operating temperatures. The liquid atomizing device should be able to deliver droplets of certain mean diameter with narrow size distribution and be able to operate within the certain flow rate range, as the flow rate may become the parameter used to control the process. The liquid delivery system should have a short response time and work in a stable fashion during transitions from one flow rate to another.

Drying of aqueous solutions involves evaporation of water and it is desirable that the radiation energy delivery should be efficient at the wavelength where the water absorption of infrared radiation is highest. Water radiation absorption has peaks at a radiation wavelength of about 3 micrometers. Therefore, the conditions of infrared heating should be such that the energy delivery efficiency reaches maximum for this wavelength. Heater temperature should be about 850 C for maximum radiation intensity at 3 micrometer wavelength. Surface emissivity should be as high as practically possible, e.g. above 0.8. To reduce actual surface temperature in contact with the product, an IR transparent, cooled window can be applied between the heater and product. Further details on infrared heating are provided in the report by Wisniewski [2014].

F.3. Liquid atomization

Small convection spray dryers and radiation/convection aerosol flow reactors typically operate with droplet sizes in the range between 1 and 25 micrometers. Liquid atomizing devices can be based on a high pressure-high velocity liquid film breakup, on a multi-fluid spraying with gas at high velocity atomizing the liquid sheet, or on vibrating devices using sonic or ultrasonic frequency.

Small convection spray dryers often use two-fluid, gas-liquid nozzles. Such nozzles can produce droplets with diameters smaller than 20 micrometers. Control of droplet size may depend mostly on the mass ratio of the atomization gas flow rate to the liquid flow rate [Masters, 1991]. Gas-to-liquid mass flow rate ratio should be minimized, yet to obtain fine droplets velocity in the nozzle can be high – fine droplets can be obtained at gas velocities exceeding 35 m/sec. Thybo et al. [2008] measured droplet size from two-fluid nozzles for a purpose of spray dryer scale up. The two nozzles that are used in spray drying were investigated. The droplet mean diameters were in the range 5-20 micrometers. The authors concluded that scaling up the nozzle using the mass ratio of the gas flow rate to the liquid flow rate may not be possible and one needs to consider the gas velocity as well. A small nozzle with film thickness of water about 0.1 mm, air velocity about 40 m/sec and gas to liquid ratio 1.0 may provide droplet size close to 10-12 micrometer [Omer, Ashgriz, 2011]. Spray parameters also depend on nozzle design and geometry [Shafaee et al., 2011]. Kemp et al. [2011] investigated atomization and spray drying using a two-fluid nozzle. Particles as small as 2-3 micrometers could be obtained if the atomizing gas to liquid ratio exceeds 6. The authors suggested that gas velocity may be the main factor in obtaining fine droplets – at gas velocities above 300 m/s droplets as small as 5 micrometers were obtained, while at gas velocity 90 m/s the droplet size was 28 micrometers. Increase in solution concentration led to larger particle size. Pre-filming air blast atomizers are used in fuel injection in gas turbines. A thin liquid film is formed on a solid surface with high velocity gas flowing above the film. Film is accelerated by gas flow and breaks at the edge of the solid surface into droplets. The gas velocities could be higher than 70 m/s [Inamura et al., 2012].

Depending on nozzle geometry, achieving a supersonic gas flow is possible. Park et al. [1996] compared performance of subsonic and supersonic nozzles. Both nozzles provided droplet size as small as 8-10 micrometers. A multi-fluid spray nozzle [Figure 8] by Fujisaki Electric company [Fujisaki Electric literature] uses gas jets to accelerate liquid film to a collision point where film breaks into fine droplets. This nozzle can produce particles of 3-5 micrometer size. This type of nozzle is described in the US Patent US005845846 owned by Fujisaki: the patent states that gas jets reach a supersonic speed and high frequency aerodynamic oscillations form after the collision focal spot and very fine droplets are formed by shock waves. The high velocity jet produced by this nozzle may require a taller drying chamber.

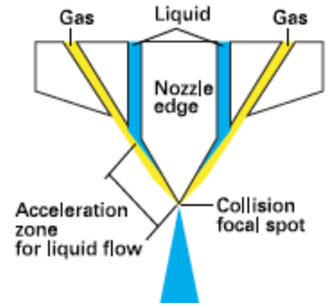

Figure 8. Multi-fluid spray nozzle with liquid film acceleration by high velocity gas [Fujisaki Electric].

Mizoe et al. [2008] reported on using such nozzle for production of inhalable mannitol microparticles containing Rifampicin. Each liquid channel contained a different liquid: aqueous solution of mannitol and organic solvent solution of the drug. Mean diameters of particles were 3.2, 3.8 and 4.0 micrometers depending on the ratio of drug to mannitol. This work demonstrated that the nozzle can be used for one step particle production using different solutes and different solvents.

Gas-liquid spray nozzles with a hollow-cone spray pattern are available with capacities from 1 to 100 L/hr, for example from Ikeuchi company [Ikeuchi Co. company literature]. Gas-liquid spray nozzles may be considered less convenient since a high pressure gas is needed for liquid dispersion, yet they can produce small droplet size. A local compressor may be added to spray dryer system [Figure 3] and may operate in an open or closed system.

High velocity swirling liquid nozzles may not be able to produce very fine droplets. For example, a small nozzle with hollow cone spray pattern made by Ikeuchi Co. can produce droplets of 35 micrometer mean diameter at liquid pressure 0.5 MPa and liquid flow rate 1.13 L/hr. Such nozzles may require drying chamber geometry design to account for longer droplet drying time and spray ejection velocity.

A characteristic number used in high pressure and multi-fluid droplet generation is the Weber Number (We). It describes the ratio between deforming inertial forces and stabilizing cohesive forces for flowing liquids. The Weber Number has been used to estimate liquid breakup into droplets.

$We = \rho_g * u^2 * D_d / T_s$; where: ρ_g is gas density, u is gas velocity, D_d is droplet diameter, and Ts is surface tension.

However, the Weber Number does not consider viscosity effect. The Ohnesorge Number (Oh) includes liquid viscosity.

$Oh = \mu_l/(D_d * \rho_l * T_s)^{0.5}$; where: μ_l is liquid viscosity; ρ_l is liquid density; T_s is surface tension and D_d is droplet size.

The studies using We and Oh numbers usually involve larger droplets breakup into smaller droplets. Droplet can break above the critical Weber Number. At low Oh numbers, the critical We number remains almost constant and is at, or above 12 (often given as 10-14 for air-water, but some reported numbers were above 20). At Oh Number larger than 0.1 and increasing, the critical We Number also increases [Sher and Sher, 2012]. The relationship between We and Oh also depends on a ratio of gas density to liquid density. Adiga et al. [2007] reviewed water droplet breakup energies and formation of very fine mist. They listed various droplet breakup mechanisms and the corresponding Weber Numbers. Vibration droplet breakup may occur at We<12; bag breakup at 12<We<50; bag and stamen breakup at 50<We<100 and sheet stripping at 100<We<350. Breakup energy to fragment 500 micrometer droplet into droplets of 23 micrometer size was18 J/kg.

For high pressure liquid nozzles, the Weber Number is sometimes based on liquid velocity in the nozzle and nozzle diameter. Such approach can result in very high Weber Numbers in the order of a few thousands that cannot be compared with results where droplet sizes are used. Indeed, liquid high velocity rotation in the nozzle causes formation of thin film in form of a cone that breaks apart into droplets. Liquid velocity and thickness of this film can be parameters used for the Weber Number, however, thickness of the film may be difficult to estimate.

The ultrasonic vibrating devices are popular in small spray dryer and aerosol flow reactor designs as they do not produce high velocity jets that enter the dryer or reactor chamber, and thus chamber geometry may depend mostly on process kinetics with only some consideration, given to the inlet droplet velocity produced by the atomizing device. Ultrasonic droplet generation devices can produce fine droplets that behave like aerosols [Fuchs, 1989], unlike the rotating wheels or high pressure spraying nozzles that produce droplets that are larger and easily settle under gravity. Ultrasonic devices can be based either on a vibrating disk or on a vibrating tip of the nozzle. Droplet size can be related to the frequency of vibration.

Vibrating disks are of a submerged type with certain liquid layer thickness required between the disk and gas-liquid interface. The vibrating disk produces jetting over the gas-liquid interface with a coarse liquid jet and large droplets ejected above the interface and then falling back into liquid under gravity. Fine droplets form on the sides of the ejected jet and form a mist cloud ("fog"), which can be then moved by the carrier gas and transported into the reactor for subsequent processing. Vibrating disk operation in this configuration depends on gravity (liquid jet and coarse droplets fall back into liquid bulk). Droplet diameter may be estimated using the following equation [Phanphanit, Cooper, 2008]:

$$D_d = 0.73 * (T_s / \rho * f^2)^{0.33} \tag{4}$$

Where T_s is surface tension, ρ is density and f is frequency. Disk vibration is typically in the frequency range 1-2.5 MHz.

An example of specifications of the piezoelectric disk used for nebulization: resonance frequency: 1.65 MHz; impedance: 2.0 ohm; capacitance: 2,000 pF; disk diameter (exposed to liquid): 16 mm; liquid level 45 mm; power 30 W; atomizing quantity (water): 0.4 L/hr; operational life more than 6,000 hrs.

Medical nebulizers for inhalation of drugs often incorporate features allowing nebulizer usage in changing positions. Design solutions often use a vibrating disk with a grid or mesh placed closely to the disk surface with liquid delivered into a narrow space between the disk and mesh. Droplets form depending on the pattern of mesh/grid orifices. Droplets are ejected from the orifices by vibration. Orifice size should be small enough to ensure proper pulmonary drug delivery (typically, it is at about 4 micrometer size), but may be larger for other applications. Such devices may atomize liquid in various directions and thus operate in a gravity-independent fashion. Droplet mean diameter for water can be 1-5 micrometers for the ultrasonic disk type atomizers and 15 -25 micrometers for ultrasonic nozzles. Droplet size may depend on the liquid properties and on vibration frequency of ultrasonic atomizing element. For example, an ultrasonic nozzle at frequency 120 kHz can deliver water droplets with mean diameter around 16-18 micrometers [Sono-Tek, Inc.].

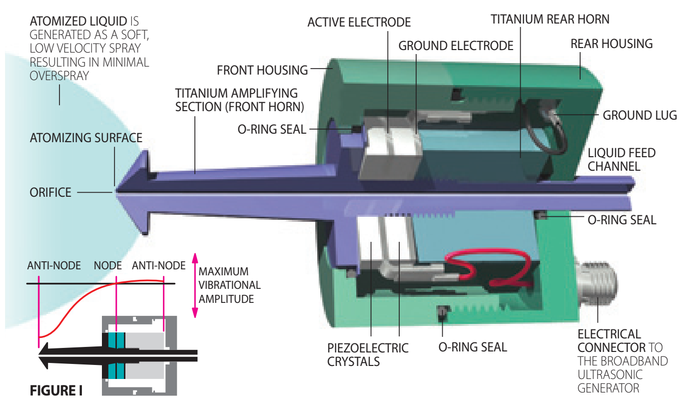

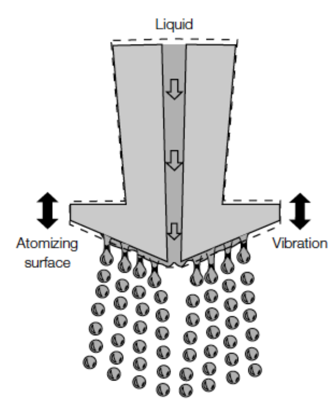

a) **b)**

Figure 9. a) Ultrasonic spraying nozzle [Sono-Tek, Inc]; b) Droplet formation [BUCHI].

Figure 9 shows an example of the ultrasonic spraying nozzle [Sono-Tek company literature] and droplet formation. Liquid is delivered by a small peristaltic pump through the central channel to the nozzle tip, where liquid forms a film, which then breaks up into fine droplets due to tip vibration. The ultrasonic nozzle can atomize liquid over large range of feed delivery rate, for example, within the range of 40-100% of the nominal rate. This makes such nozzle suitable to be used in a control scheme with controlling variable being the liquid delivery rate, for example, to maintain the dryer outlet gas temperature at preset level. Ultrasonic nozzle can spray vertically or horizontally in a gravity-independent operation. Droplets are ejected with low velocity suitable for designing a compact drying chamber. An advantage of the ultrasonic nozzles is that a low pressure liquid delivery pump can be sufficient. In general, such nozzle may produce larger droplets than the gas-liquid nozzles. Nozzle vibrational frequency may be limited due to transducer and vibrating horn design limitations. Dalmoro et al. [2013] reviewed ultrasonic atomization approaches for the drug delivery microsystems. The authors proposed the following correlation for droplet diameter using ultrasonic atomization:

$$D_d = 0.058*(\pi*T_s/(\rho*f^2))^{0.33} *(We)^{0.151} *(Oh)^{0.192} *(I_N)^{-0.02} \quad (5)$$

Where I_N is Intensity Number; $I_N = f^2 *Am^4 /(C*Q)$; Am is amplitude, C is speed of sound , Q is flow rate and f is frequency. Modified Weber and Ohnesorge Numbers are as follows: $We = f*Q*\rho/T_s$; $Oh = \mu/(f*Am^2 *\rho)$.

The BUCHI B-90 Nano spray dryer uses a unique ultrasonic spraying device – a vibrating disk with orifices that control the droplet size [Figure 10]. There are heads available with different orifice sizes (the smallest orifice size is 4.0 micrometers, other heads have 5.5 and 7.0 micrometer orifices). This design has been employed to obtain nano- and micro-particles. Feed liquid needs to be filtered to prevent orifice plugging. The BUCHI B-290 Mini spray dryer may use a gas-liquid spraying nozzle or an ultrasonic nozzle similar to the Sono-Tek design. The Yamato Scientific ADL311, Keison D-05/06 and Fujisaki spray dryers use gas-liquid spraying nozzles.

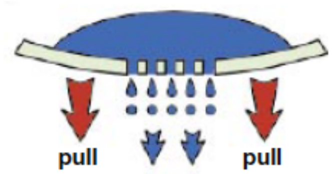

Figure 10. BUCHI B-90 droplet generator [BUCHI].

Droplet size may be a factor in operation of the dryer regarding wetting of system surfaces. Droplets smaller than 12-15 micrometers might bounce off solid surfaces (so called "dry fog" conditions). In practice, "dry fog" generators use droplets smaller than 10 micrometers. Droplets larger than 20 micrometers may cause surface wetting (within droplet size range between 20 and 60 micrometers, called "wet fog" and fine mist). This can make an important difference in the convection dryers if the stream of drying air brings droplets close to the drying chamber wall. By design, in the convection dryers, droplet evaporation and drying may occur in the chamber volume without droplet contact with the walls. This phenomenon may be more critical in the radiation-convection dryers where droplets might get into contact with a hot surface of radiation heater. Therefore, devices that generate droplets below 15 micrometers may be preferred. Typical ultrasonic spray nozzles produce larger droplets than vibrating disks, thus nozzles with the highest available frequency may be considered. Small capacity ultrasonic devices may produce fine droplets, for example, ultrasonic nebulizers for inhalation drug delivery may produce droplets in the range 2-5 micrometers [Tsai et al., 2013]. Huang et al. [2014] compared 3 commercial ultrasonic medical nebulizers with 3 jet nebulizers. The tested drugs were bonsetan, pirfenidone, treprostinil and sidenafil. The jet nebulizers used 35 psi gas pressure. The ultrasonic nebulizers operated under 2.4 and 2.5 MHz frequencies. The ultrasonic nebulizers produced mean droplet sizes 2.7, 3.5 and 3.7 micrometers. The jet nebulizers produced mean droplet sizes within the range between 2.3 and 4.5 micrometers depending on the drug and residual cup size. Alvarez et al. [2007] designed an atomizer based on the surface acoustic wave principle in attempt to produce monodisperse aerosol and particles for drug delivery. Insulin droplets of 4 micrometers were produced – this droplet size was considered optimal for maximizing droplet absorption in the lung alveoli. Polymer particles of 130-220 nm were obtained using evaporation and nucleation process. The surface acoustic wave devices had frequencies 8.6 MHz and 19.3 MHz.

Droplet generation concept might be adapted from fog-making devices if the vibrating disk reliability is a concern. Fog-making devices can generate fog with droplets smaller than 5 micrometers. An example can be a fog generator by Fogmaster [Fogmaster company literature]. It uses a counter rotating high shear fogging nozzle that can generate droplets smaller than 5 micrometers. A blower that generates turbulent air stream is a part of this device. Liquid flow rate controls the fog characteristics and droplet size. Flow rate rates of 30-60 mL/min. produce dry fog with droplets below 10 micrometers. Increase in the liquid flow rate will produce larger droplets. Liquid flow rate is adjusted using a control valve. There are many similar products on the market, typically called "cold foggers". Such generators capacity might exceed requirements of aerosol flow reactors, but a smaller device can be constructed using these principles. High pressure nozzles of special design may also be used to generate fog. Chaker et al. [2002] investigated two designs of high pressure nozzles: swirl and impaction-pin types. The nozzles operated at high pressure (137 bar) and could produce droplets in the 10-20 micrometer range. Increasing liquid pressure from 103 bar to 138 bar resulted in decrease of droplet size, but for pressures above 138 bar there was no significant droplet size change. There are droplet generators, that can electrostatically charge the droplets. This may reduce droplet coalescence as well as alter the spray shape. Charged fogs are used in reduction of fine particulate pollution and in agricultural spraying. Murata et al. [2008] described a dry fog ionizer. It was based on a dry fog nozzle made by Ikeuchi company. A ring electrode was placed in front of the nozzle for fog induction charging. Fan was added to disperse charged fog. The nozzle produced droplets with 8 micrometer diameter. Applied voltage was 5 kV and density of ionic space charge was approaching 1,800 nC/m^3 at 2 m distance from the nozzle. Drying of charged droplets is possible and charge may reduce droplet coalescence and facilitate particle separation – further research with spray dryers and aerosol flow reactors may be conducted. Fog droplet size and wall wetting may also depend on liquid properties. As a result, the generator may produce dry fog for some liquids, but may produce droplets approaching wetting range for others. Therefore, for processing various liquids, or a liquid with varying properties, dryer surfaces may be modified, for example, made more hydrophobic.

In general, nozzle selection may require help from the nozzle manufacturers, as well as an experimental work. Experimental work with processed liquid is required since nozzle data typically are provided for water, or for simple fluids or solutions.

F.4. Particle separation

F.4.1. Particle separation in convection-based spray dryers

Convection spray dryers use large quantities of air that flows through the system, drying and transporting droplets and particles. A particle separation device has to be designed to match the high air flow rate, particle load and particle size distribution. Practical separator designs used in small spray dryers are of a dynamic type in form of cyclone. Cyclones are usually followed by a filter to capture the finest particles. Separation of particles can take place in a rotational flow under both, 1 g and microgravity conditions. Particle discharge from cyclone is through the bottom cone and depends on gravity. Such cyclones may not be applied in microgravity in their original form. Particle removal from the cyclone needs to be adapted for microgravity conditions. It is possible to operate the traditional cyclone design under reduced gravity. Crosby et al. [2008] reported on cyclone performance under reduced gravity for separation of lunar dust under the Moon gravity field. Experiments in parabolic flights and CFD simulations indicated that there was no significant difference in the separation efficiency between the 1 g and reduced gravity conditions.

A modification of the cyclone concept may be considered, for example, an axial cyclone design with radial or tangential ejection of collected particles into an external collection chamber. Axial flow cyclones can be designed and operated to have equivalent or even better performance than the conventional tangential flow cyclones [Vaughan, 1988]. They can provide separation efficiencies close to 100% for particles larger than 2-3 micrometers. Recent axial cyclone designs can provide high efficiency separation for particle sizes below 1,000 nm [Hsiao et al., 2011]. A multi-stage axial flow cyclone may be able to separate particles below 100 nm [Hsiao et al., 2010]. Cyclone may be followed by a filter to capture the remaining fines. The BUCHI Mini B-290, Yamato Scientific ADL311 and Keison SD-05/06 dryers all use the cyclone particle separators with tangential inlet.

Another option is to capture particles in a filter. Filter sizing should consider the air flow rate, particle size distribution and particle load. Filters typically follow the cyclone or other separator, but they can be used alone – for example, Fujisaki Electric offers laboratory spray dryers with a bag filter, as well as with cyclone followed by a bag filter [Figures 7 and 8].

Industrial designs of dust/particle separators also employ electrostatic forces. Electrostatic precipitators (ESP) operate using high DC voltage – low current principle, and particles are collected on one electrode. DC voltage can be within the range of 15-100 kV. Gas stream with suspended particles passes between the parallel plates or through cylindrical electrodes. Particles moving with the gas stream are subjected to intense bombardment by the negative ions and become highly charged in a very short time. Typically, a 1 micrometer particle can carry about 300 electron charges, whereas10 micrometer particle may carry about 30,000 electron charges [Yuan, Shen, 2004]. The particle-charging mechanisms are as follows: field charging with particles bombarded by ions moving under the influence of the applied electric field; diffusion charging, with particles being charged by motion of the ions produced by the thermal motion of surrounding gas molecules. The field charging mechanism works mostly for the particles larger than 0.5 micrometer, and the diffusion charging mechanism works mostly for the particles smaller than 0.1 micrometer. Particles with sizes between 0.2 and 0.4 micrometers can be more difficult to capture in electrostatic precipitators. Performance of electrostatic precipitator also depends on the gas velocity and on electric field – it decreases with increase of gas velocity and increases with increase of electric field strength [Nobrega et al., 2004].

Operation and performance of the electrostatic precipitator depend on particle resistivity. The best range of resistivity for particle collection in electrostatic precipitators is 10^{7} –10^{10} Ω -cm. Typical power density of electric field where separation takes place can be around 10-20 W/m^2, and for high resistivity dusts between 1 and 5 W/m^2. Particle collection efficiency can be very high (above 99%) and may decrease for particles below 1 micrometer if their concentration is high [Neundorfer, Inc., company literature]. These devices may require low gas velocity in space between the electrodes, usually less than 1.0-1.6 m/sec. with lower velocities preferred, thus for high air flow rates the electrostatic precipitator dimensions can be larger than the cyclone separator size. An electrostatic precipitator can efficiently operate at very low air flow rates where cyclone may have poor separation efficiency. Particle collection efficiency of ESP decreases as the discharging electrode and collection plates get contaminated with particulates. When the layer of dust on the collection plate increases, the collection efficiency decreases because a back corona occurs in the deposited dust layer. Layers of dust particles that accumulate on the electrode produce a resistance in flow of ionic current toward the collecting plate. When the ionic current passes through the dust layer to reach the electrode, this ionic current produces an electric field in the layer. At a large enough electric field a local breakdown may occur. When this happens, new ions of wrong polarities are injected into the electrode-plate space where they reduce charge on particles and cause sparking. This is called back corona. Wrong polarities ions are positive ions, and these positive ions tend to move toward electrode that is creating the main corona. Moving toward the corona electrode, these positive ions collide with the negative ions that are moving toward the collecting plate, and reduce the overall field strength. This effect is detrimental to efficiency of the ESP and must be avoided to save power and to maintain high value of electric field and current density to obtain maximum separation efficiency. The BUCHI Nano dryer B-90 uses an electrostatic precipitator for separation of particles [Figure 11]. Solid particles build up a layer on the collecting electrode surface, from which the accumulated deposit has to be periodically removed. This is accomplished in the industrial designs by shaking, vibration, rapping or flushing. In practical applications, the dust layer thickness may reach between 5 and 25 mm before electrode cleaning is applied. Released particles fall into a hopper. Such plate cleaning may not work in microgravity, therefore, other methods of particle collection from electrodes need to be devised. For example, in a batch operation, a piston type pusher may scrap and compact the particles after each run, or the electrode with particles may be moved out into a container.

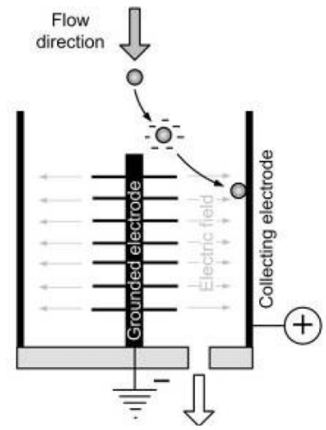

Figure 11. Electrostatic precipitator in the B-90 Nano dryer [BUCHI].

F.4.2. Particle separation in radiation/convection reactors

Particles produced in a dryer need to be separated from the carrier gas. Due to low quantity of the carrier gas, dynamic separators using high velocity gas stream may be impractical. Therefore, electrostatic precipitators and membrane or cloth filters may be considered. Electrostatic precipitators may work well, but for microgravity operation, methods of unloading the collected dust need to be devised. The aerosol drying apparatus at NASA Ames [Umpqua Research Co.] uses the electrostatic precipitator for particle separation.

Filter capacity needs to be considered to last for batch time without experiencing too high pressure difference across the filter membrane and layer of collected solids. A combination of electrostatic precipitator and final filter may be used. The filter will be only used to trap the traces of fine particles that might pass through the precipitator.

G. Process dynamics and control

Spray drying is considered a rapid process with droplet drying times on the order of a few seconds in the large industrial installations and around 1 second in laboratory systems. This is because of relatively large droplets are generated in large systems (the droplets can be larger than 100 micrometers) and due to differences in air and droplets flow patterns inside the drying chamber. In the small dryers where droplets can be dried very rapidly, product quality may be affected by system and controls dynamics. Since drying is a thermal process, system thermal dynamics plays an important role, but dynamics of subsystems can also affect dryers' performance.

Particle-producing systems using drying of droplets may be approximated by system models of first order with time delay type. Since system operates with short droplet residence time, therefore time delay for processed material is short. System dynamics can be dictated by design of controls and operation optimization. Due to short time delays, controls response time has to be fast. Typical modeling approaches use thermal dynamics of the process. Since particles follow carrier gas streamlines and may reach gas temperature in the dryers' outlet, measurement of the outlet gas temperature maybe used as a control parameter. Thermal delay time is thus caused by gas and particles residence time in the system and can also be affected by thermal properties of the dryer (its structural mass, heat transfer between walls and gas and product, heat losses to environment). A general approach to process dynamics analysis that is used in processing industries can be employed (Seborg et al., 1989; Luyben, 1996, Clark 1996). System characterization may involve empirical results of operating system being disturbed by a step change in the inlet parameter and monitoring the system corresponding outlet parameter [Liu et al., 2013]. System response is then analyzed and a model developed [Bohlin, 1991].

G.1. Convection-based spray dryers

Convection spray dryers can be in general, represented by the first order process with time delay model. The transfer function of the drying plant can be represented by the formula: G(s) = K * exp (-T_d * s)/(T_c *s + 1); where: K is gain; T_d is time constant; T_d is time delay. Tan et al. [Tan et al., 2010, 2011] studied spray drying process and system dynamics using the LabPlant SD-05 spray dryer. Such studies may provide information that can be used in the system control scheme including tuning of controllers. Model of such system dynamics may be represented using a block diagram. Model using software package Scilab/Xcos is shown in Figure 12a.

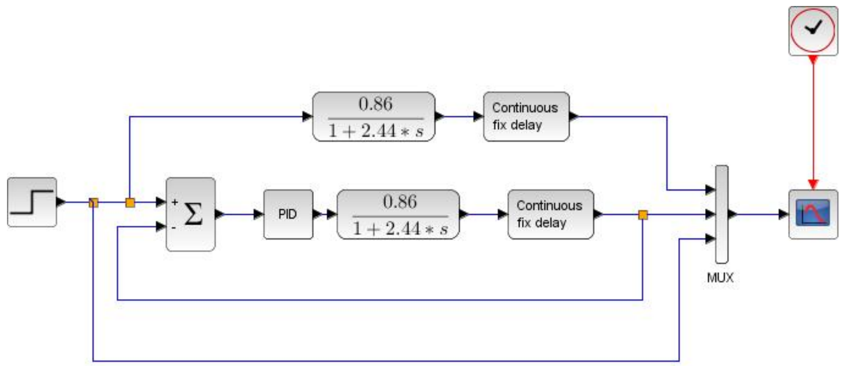

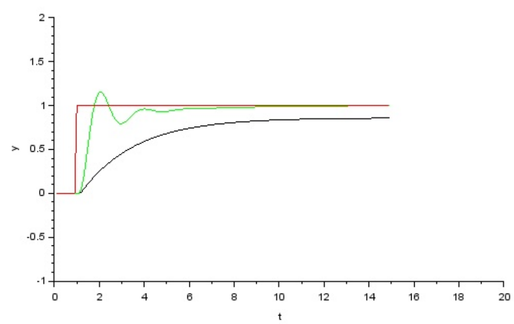

a) **b)**

Figure 12. a) Block diagram of process using Scilab/Xcos for SD-05 spray dryer; data by Tan et al. [2010, 2011]; a PID controller has been added for this model. b) Spray dryer dynamic response to step change in inlet air temperature ; red-step change; black -system dynamic response without control; green-system dynamic response using PID control. Y is signal, t is time.

This block model combines the system dynamic response and system response using a PID controller. Transfer function uses the data reported by Tan et al. [2010,2011]. System dynamic response to a step interference is shown in Figure 12b. Step change is applied to the inlet air temperature and response is the outlet air temperature. The PID controller parameters were estimated using the Matlab/Simulink PID controller tuning tool. These parameters were as follows: P= 3.68, I=1.40, D=-1.68.

Control methodology and control system design have been well established for the convection spray dryers using extensive industrial experience. Simple control schemes use the dryer outlet air parameters to control the process, controlled variable being the liquid feed delivery rate. Figure 13 shows an example of controls with possible instrumentation options.

System dynamics can be lumped together if the system is small and subsystems dynamics do not introduce large delays. Such approach is represented in Figure 12. If the subsystems introduce significant dynamic effects and time delays, then the system control concept needs to consider those factors. A single PID controller may, or may not be sufficient to deliver adequate system performance. For example, liquid delivery to the atomizing device can be controlled by the outlet air temperature but it could have such dynamics and time delay that overall system performance can be affected (feed subsystem factors: preheating of liquid feed, length of feed line, pumping system dynamics, pump performance). The example shown in Figure 12 may have such subsystem dynamics and time delay added [Figure14]. System and subsystem dynamic responses to step interference are shown in Figure 15. Two different sets of P and I controller parameters are shown.

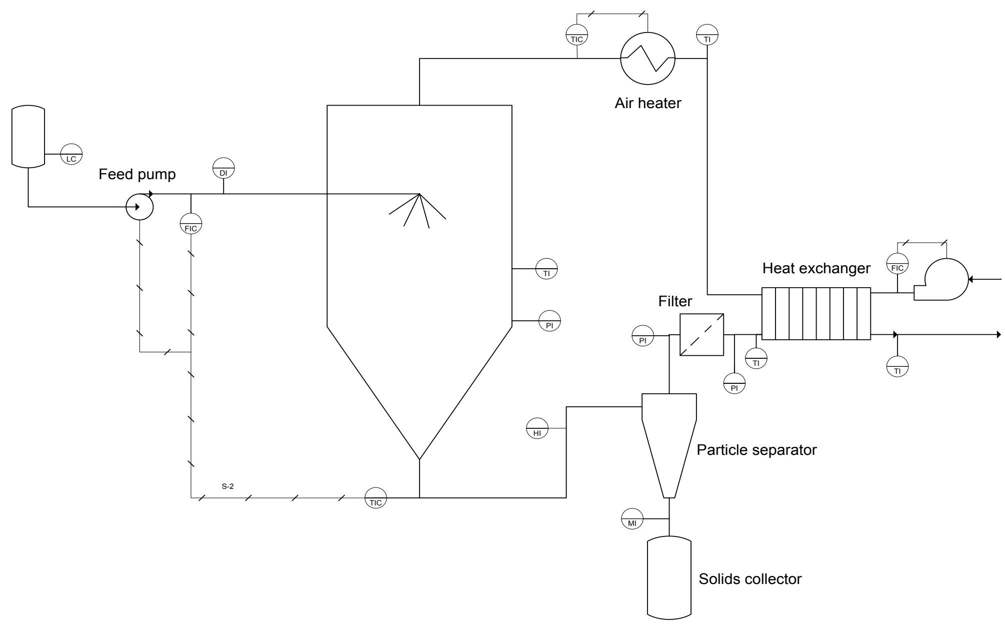

Figure 13. Example of controls of convection spray dryer.

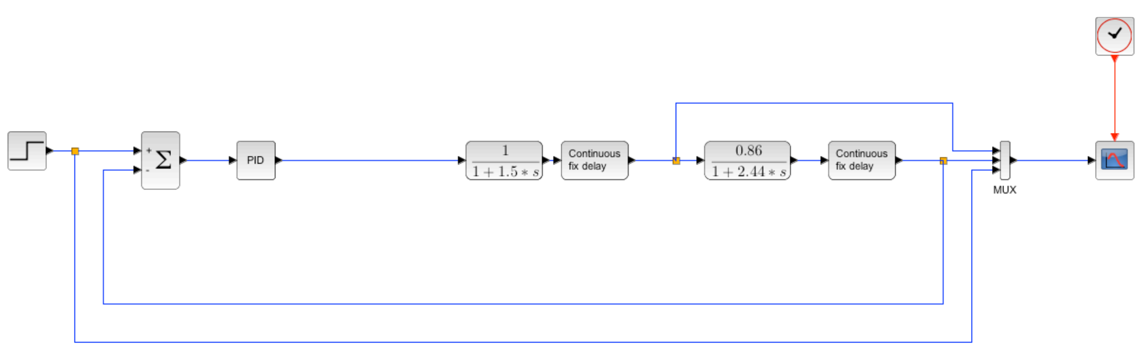

Figure 14. Block diagram of process using Scilab/Xcos – additional subsystem dynamics and time delay has been introduced.

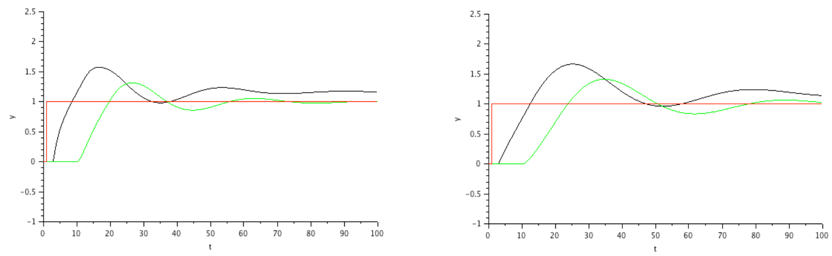

a) **b)**

Figure 15. System dynamic response to step interference using a single PID controller. Green – overall system response; black – additional subsystem response; a) P=0.3, I=0.1; b) P=0.6, I=0.1.

Industrial spray dryers often operate together with multi-effect falling film evaporators. Evaporator final control element can be a density meter that monitors solids concentration after the evaporator. In the case of coupled systems: evaporator – spray dryer, such density meter can also serve as a control element for the dryer since it provides information on water content in the dryer feed to be evaporated in the dryer. Density meter can also be combined in one instrument with a mass flow meter, using a vibrating tube and based on the Coriolis effect [Emerson/Micro Motion company literature]. Accuracy of such instrument can be about $\pm$0.15%. Since this is the information on feed at the dryer inlet, it can be used in various control schemes, for example in a model-based control, or in a feedforward control. The model-based control and feedforward control require development of process models. This may not be initially possible. Veronesi and Visioli [2013] proposed a method for design of feedforward compensator for the PID control loop and automatic tuning. Parameters of the compensator are computed from the first response to disturbance by the PID controller.

A scheme of advanced control concept that may not require models may be a cascade control using two PID controllers [Cooper, 2004]. Methods of tuning the PID controllers in the cascade scheme are available [Thomas, 2007; Visioli, Piazzi, 2006; Veronesi, Visioli, 2011]. The cascade control scheme may improve control performance if the inner control loop responds faster than the outer control loop. In general, if there is a speed difference between the inner and outer loops, one may consider using P or PI controllers only. If the inner process is less than 3 times faster than the whole process, a P controller may be considered. If the inner process is more than 5 times faster than the whole process, a PI controller may be considered [Cooper, 2007]. For example, the cascade scheme may be considered if the liquid feed pump has nonlinear characteristics regarding delivered flow rate, depending on rotational speed and backpressure. Industrial dryers that use rotary atomizers do not require high pressure pumps and may use a positive displacement or a centrifugal pump. Positive displacement pumps are used with high pressure liquid nozzles. For example, a piston or plunger pump with multiple heads may be employed. High pressure nozzles may wear off or plug, thus changing the spray characteristics in the dyer if multiple nozzles are used. Small dryers typically use one nozzle, thus nozzle plugging may be detected. Dryers with gas-liquid nozzles require pump that can deliver against pressure that occurs in the nozzle. An additional parameter is the gas flow rate and its pressure – variations may cause changes in spray pattern and droplet size, and affect the drying process. A liquid flow control loop with feedback using a flowmeter may be added. Figure 16 shows an example of possible cascade control scheme of the convection spray dryer. The inner liquid delivery loop may respond faster than the outer thermal loop of the dryer. This development is based on the concept shown in Figure 14.

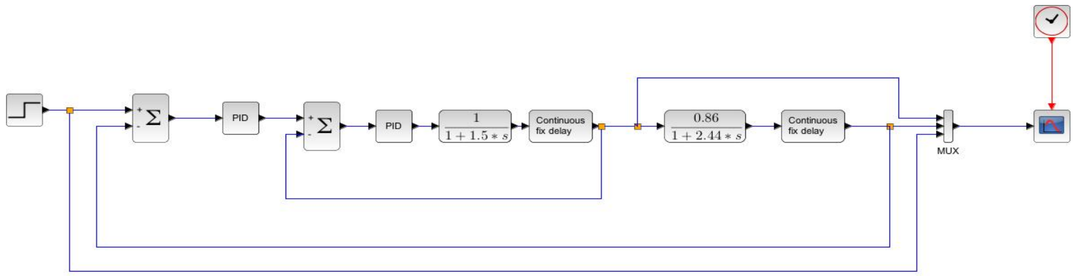

Figure 16. Cascade control scheme of convection spray dryer. Inner loop is the feed liquid delivery loop; outer loop is the thermal loop; using Scilab/Xcos.

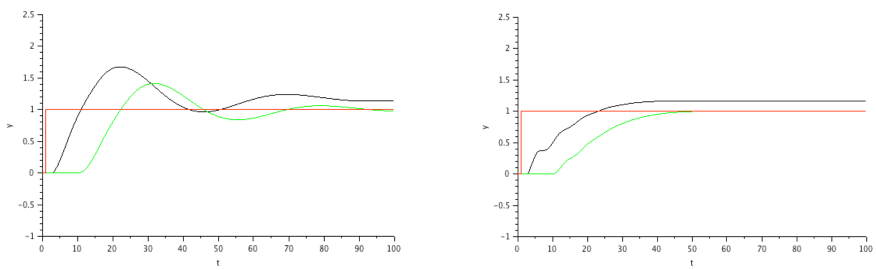

a) **b)**

Figure 17. System dynamic response to step interference using two PID controllers in cascade configuration. Green – overall system response; black – additional subsystem response; a) Inner loop P=0.3, I=0.3; outer loop P=0.3, I=0.1. b) Inner loop P=1.2, I=0; outer loop P=0.2, I=0.1.

Cascade configuration benefits may depend on tuning of the inner and outer loop controllers. Figure 17a shows a trend similar to the case with a single PID controller, but changing the tuning parameters could improve the process [Figure 17b].

These are simplified illustrative examples and real system dynamics and time delays may involve multiple subsystems contributing to the overall system performance.

G.1.1. Liquid properties

Liquid properties may determine droplet generation process and droplet size. Droplet size may depend on liquid surface tension and viscosity. In-line liquid viscosity sensors based on vibrating elements are available (for example, using vibrating forks [Emerson/ Micro Motion company literature]). Vibrating sensors of fork, cantilever, plate or membrane type may be used to simultaneously measure density and viscosity [Abdallah et al., 2014; Takarada et al., 2012].

Typical surface tension meters are bench instruments that can measure surface tension of liquid samples. Surface tension meters that might be used in-line are based on a principle of gas bubble formation. For example, the SensaDyne surface tension meter [M&H Technologies company literature] is based on generation of gas bubbles through 2 or 3 orifices (0.5 mm, 1.0 mm and 4.0 mm) and using differential pressure of bubble formation. Measurement accuracy can be $\pm$ 0.1 dyne/cm. M&H Technologies company offers the on-line (in-process) surface tension meter, model IP6000. Other sensor makers use a single orifice bubble generation. This type of surface tension meter may need to be located after the vibrating instruments for flow, density and viscosity, since the gas bubbles may affect their reading. Gas bubbles may interact with droplet formation – in such case, a gas-liquid separator may be considered prior to the droplet generator. Introduction of gas bubbles into sprayed liquid may also enhance liquid atomization in the process called effervescent atomization [Sovani et al., 2001]. Kramer et al. [2012] reported on using the SensaDyne surface tensiometer in optimization of flotation control in the industrial plant. There was a relation between separation efficiency and surface tension of the slurry with an optimum operating point that maximizes separation efficiency. Surface tension plays a significant role in microscale processes, for example in microfluidic devices. Therefore, it is possible to construct a microfluidic sensor for measurement of gas-liquid interface tension. Nguyen et al. [2007] reported on interfacial tension measurement using an optofluidic sensor. The principle was gas bubble injection into the liquid flowing through a capillary.

These liquid properties may be related to droplet formation and droplet evaporation, yet direct measurement of the spray quality and spray evaporation would be desirable. Optical methods have been used for the spray characterization. An example can be the Spraytec system for the spray droplet size measurement [Malvern company literature]. This instrument uses the technique of laser diffraction for size measurement of spray droplets and spray particles. It does this by measuring the intensity of light scattered as a laser beam passes through the spray. This data is then analyzed to calculate size of the droplets that created the scattering pattern. It is being used for characterization of sprays produced by atomizers, nozzles, nebulizers and aerosol generators. Hardalupas et al. [2010] proposed a novel approach to measurement of evaporative sprays: the Interferometric Laser Imaging Droplet Sizing (ILIDS) in combination with Laser Induced Fluorescence (LIF). Measurements were conducted for mono-sized droplet streams for two droplet sizes. Vapor surrounding the droplets was also investigated. However, this or similar methods may not be ready yet to be applied in spray dryers for routine operation.

G.1.2. Solids properties

Some powders may be sensitive to a relative humidity (RH) of air. Air humidity is usually sensed in the dryers' outlet air stream. The changes in relative and absolute humidity can be monitored in the outlet air using a hygrometric humidity sensor. Schuck et al. [2005] investigated a thermohygrometric sensor for optimizing operation of the spray dryer. Sensor could measure absolute and relative air humidity in the outlet air stream. Dairy products were investigated: whole milk, skim milk and whey were spray dried. To avoid powder sticking to the walls near the dryer bottom, relative humidities of outlet air should not be higher than 11% for the whole milk powder and no higher than 7% for skim milk and whey powders. Changes in outlet air humidity may result from changes in absolute humidity of inlet air, total solid content of concentrate, crystallization rate, and outlet air temperature. An increase in the outlet air humidity may increase powder stickiness. Control system concept may include scheme that uses not only the outlet air temperature, but also outlet air humidity. Schuck et al. [2008] reported that the relative humidity of outlet air can be a key parameter to optimize moisture content and water activity of dairy powders. For example, the moisture content of skim milk powder should not be higher than about 5%. The authors found no clear relationship between the powder moisture content and outlet air temperature. Outlet air relative humidity was found to be directly related to the powder moisture content: for example, at the air relative humidity of 7%, the powder moisture content was 5.1%. Gianfrancesco et al. [2008] investigated air properties inside the spray drying chamber and its effects on powder agglomeration. They measured air temperature and relative humidity in multiple points in the drying chamber. They demonstrated that most of the drying occurs in the region close to the atomizer. There was a significant difference between the processes of evaporation of water droplets and evaporation and drying of maltodextrin solution that evaporated and dried slowed than water. With feed rate increase, at certain feed rate the drying could not be completed with particles sticking to walls – then the outlet air relative humidity approached 30%.

Sensing the air humidity in the dryer outlet can provide additional information about amount of water removed and can aid in estimating water content in the powder. Air humidity sensor should be able to operate at temperatures exceeding 100 C. The humidity range should cover the low humidity values up to approximately 40%. For example, the humidity sensor by Sensirion AG company [Sensirion company literature], model SHT31, can operate in the temperature range from -40 to +125 C and in the relative humidity range from 0 to 100%. The sensor time constant is 8 seconds. The industrial humidity transmitter by Rotronic AG company [Rotronic company literature], model XB, can operate at the temperatures up to 200 C and at the humidity range 0-100%. Accuracy is $\pm$ 1% of RH. Many reported examples of practical performance of laboratory scale convection dryers show the range of relative humidity of outlet air. One may follow these data during an early stage of process development.

Outlet air temperature and humidity can be related to powder moisture content and to possible particle stickiness, yet direct moisture content measurement in the powder could verify that the process control scheme is sound. Rapid moisture determination in the produced powder may serve for fine adjustments of the control system parameters. Corredor et al. [2011] compared near-infrared and microwave sensors for moisture determination in powders and tablets. The inquiry was about a possible replacement of the well-established laboratory method of Karl Fischer titration. The near-infrared method could accurately predict water content in bulk powders in the range of 0.5–5% w/w. Results were compared to a microwave method. The Karl Fischer titration method was used as reference. Both, the near-infrared and the microwave methods showed good agreement with the Karl Fischer method. These methods do not require sensor contact with the sample. Near-infrared radiation penetration into the powder may vary from 0.5 to 2.5 mm, and microwave penetration may be within the range of 2-5 cm. Therefore, if there are variations of moisture content in the powder bulk, the microwave method may provide more representative result. The authors used the Sartorius LMA 320PA microwave moisture analyzer that operates at the frequency of

2.5 GHz [Sartorius company literature]. While the near-infrared method requires calibration for each type of powder, the microwave method may detect moisture content in various powders (a general calibration method may be sufficient). Currently, Sartorius can deliver microwave sensors that can measure powder moisture content in on-line applications. Microwave resonance technology offers advantage of extremely fast measurements that may take a few milliseconds. This allows measurement of moisture in products that pass in front of the sensor at high velocities. One may consider a model-predictive-control approach with such parameters as outlet air temperature, outlet air relative humidity and powder moisture content to be the control parameters. Eventually the powder moisture content and the outlet air temperature may be considered. The feeding liquid stream may be controlled depending on these dryer outlet parameters. The feed liquid subsystem may have an inner control loop with a flowmeter providing feedback for the pump speed control.

The industrial dryers may be more complex systems than the scheme shown in Figure 13. For example, they may include a fluid bed dryer at the bottom of the spray drying chamber followed by a vibrating fluid bed subsystem in which agglomeration and cooling of powder may take place. Models of such systems become more complicated. Approach to modeling may be based on system identification – for example, Petersen et al. [2013] proposed a grey-box model for such multi-stage spray drying plants.

G.2. Radiation/convection spray dryer

Radiation and radiation/convection flow reactors are either treated as plug reactors, or as laminar flow reactors with a parabolic velocity profile. Plug reactor approach may be suitable for the packed beds reactors, but may not well match the empty tube reactors. Often a laminar flow of fluid is employed in reactor operation and then a reactor model with parabolic velocity profile may be used. The parabolic velocity distribution along the radius r is: $u_r = u_{max}*[1-(r/R)^2]$; $u_{max} = 2*u_{av}$ Model may assume that there is no longitudinal nor radial mixing in the reactor. Such reactor may produce distribution of residence time similar to the laminar flow without diffusional dispersion [Danckwerts, 1953]. Figure 18 shows an example of possible design of such reactor working as spray dryer. For the ideal laminar flow reactor, response to a step introduction of of tracer can be represented by function F [Figure 19] [Levenspiel, 1999]: $F = 1 - 1/4*T_e^2$; where $T_e = t/(L/u)$; t - time; L - reactor length, u - average flow velocity. This approach assumes parabolic velocity profile in the reactor tube. Flow rate of the carrier gas is controlled to maintain laminar flow and can be varied within certain range. The controlled parameter may be the liquid feed flow rate. Due to system slow thermal dynamics, heater control is based on maintaining a certain temperature profile along the reactor, whether it is constant or variable, if a multi-zone furnace is used for the reactor tube heating (in a process based on drying of fine droplets there may be a need to vary heated wall temperature

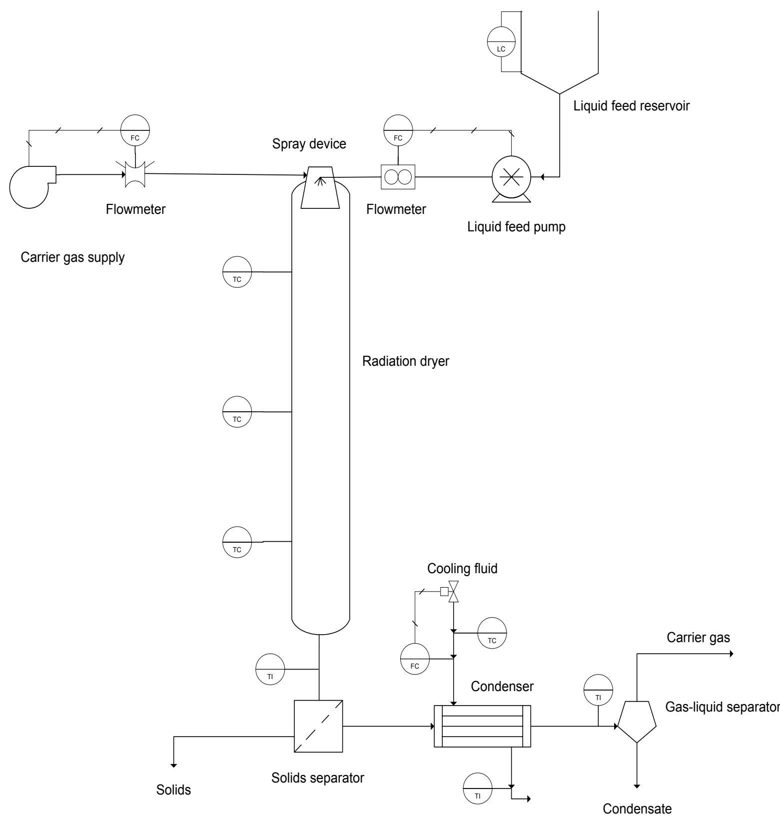

Figure 18. Radiation/convection spray dryer/reactor.

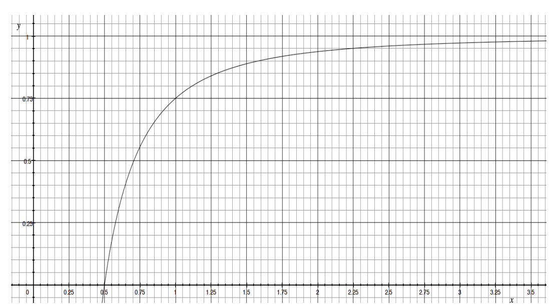

Figure 19. Function F – response to step tracer introduction.

along the reactor).

A model for the ideal laminar flow reactor considering dynamic response to tracer introduction may be formulated using Scilab/Xcos [Figure 20a].

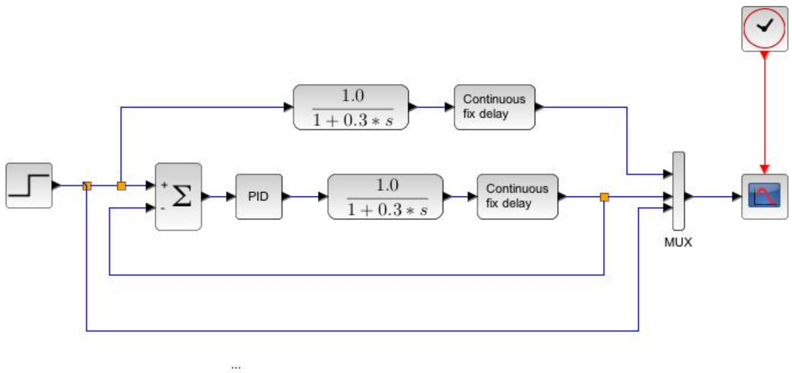

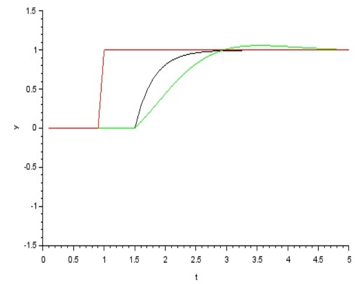

a) b)

Figure 20. a) Model of ideal laminar flow reactor using Scilab/Xcos; b) Laminar flow reactor dynamic response to step tracer introduction. Red – step change; black – system dynamic response; green – system dynamic response with a PID controller.

A response to the tracer [Figure 20b] may correspond to real events, such as change in solutes concentration sensed by a conductivity meter, or by a density meter. The first order process has been employed in this model following literature information that the spray-fed laminar thermal reactors may be approximated using models of the first order systems with time delay [Masoumi et al., 2006]. The system from Figure 20a dynamic response and the response using the feedback loop with a PID controller are shown in Figure 20b. The PID controller tuning parameters used in this example were P=0.239, I=0.926 and D=0 and were obtained using the Matlab/Simulink controller tuning tool. In this simple example, the PID controller may not provide an advantage.

Control scheme may use the outlet carrier gas temperature as a control parameter, or a monitoring signal. Masoumi et al. [2006] conducted dynamic experiments using a tubular reactor with a mixture of steam and hydrocarbons. The reactor L/D = 100 and the Reynolds number was 600. Experiments with a step change in heater voltage and checking wall temperature response showed that the system could be represented by the first order process with time delay with the transfer function as:
$G(s) = K * \exp(-T_d * s)/(T_c * s + 1)$. The reported transfer function parameters were K=125, T_c = 1,300 and T_d = 130 (times in seconds). Temperature range was 800-950 C.

Since the tubular furnace heaters can have slow thermal dynamic response, faster response may be obtained using liquid feed flow rate changes delivered by a variable speed pump to the liquid atomizer. For example, if there is a sudden solute concentration change in the feed and water content to be evaporated changes, then the outlet gas temperature may change and this signal can be used to change the feed delivery rate by changing the pump speed. If the concentration of solutes increases and thus the water evaporation mass decreases, then the outlet gas temperature would increase. This temperature increase would occur with some time delay in a pattern similar to the F function above due to the laminar flow. Feedback controller would then change liquid feed flow rate to maintain the outlet gas temperature at the desired level to avoid particle overheating and possible degradation. In the case of solutes concentration increase, the feed rate of liquid would increase to maintain the quantity of evaporated water steady.

Typical electrically-heated furnaces can have a large thermal inertia and may respond very slowly in comparison to changes in the carrier gas temperature and related amount of evaporated water. Time constants of wall temperature response to a change in heater voltage can be as long as 15-30 minutes. Time delays due to laminar flow may be acceptable for tubular reactors of short to moderate length, but may not be acceptable for feedback control for very long reactors. For example, if a tubular reactor has 100 mm internal tube diameter and reactor thermal length is 1,000 mm (L/D = 10), then at an average carrier gas velocity of 50 mm/sec, the average residence time will be 20 sec. Using the laminar flow profile, axially located temperature sensor in the outlet zone would detect the first temperature change after about 10 sec. Controller may then change the liquid feed rate to maintain the outlet gas temperature at a preset level. In this example, the results of Figure 20b above may indicate that the controller may bring a new flow rate after about 80 sec. If the flow rate of the reactor is 200 mL/hr, liquid volume passing in this transition time will be about 4.4 mL or 2.2 % of the hourly rate. At frequent variations in solutes concentration in the feed this type of control may become questionable if reactor operation temperature is close to the product degradation temperature. At these processing conditions, the heat of water evaporation would be about 455 kJ at energy delivery rate close to 127 W. Amount of water in droplets present in the tube volume will be about 1.1 mL counted as a holdup. In the aerosol flow, this may correspond to water fog density of 14.3 mL/m^3. In the reactor inlet zone, water will be in form of fine droplets and in the reactor outlet zone in form of water vapor. Transition from droplets into particles takes place firstly at the heated walls and progresses towards the tube center along the reactor. Due to the laminar velocity profile, droplets and particles at the center may experience residence time being 0.5 of the average residence time. Reactor design should ensure complete drying of the droplets in the central core near the tube axis.

For long tubular reactors, length of the time delay may become unacceptable. Control scheme may involve sensing feeding liquid properties such as water content, and it may be conducted using an in-line density meter, or a conductivity meter if conductivity is proportional to solutes concentration. A feedback from the outlet gas temperature may still be required, but its value could become questionable for long time delays. At long time delays, prediction of time delay can be implemented into the control scheme. For example, a Smith Predictor control structure has been used for systems with long time delays [Wang and Skogestad, 1993; Landau, 1995; Lee et al., 1996]. The prediction time is computed by use of the drying plant without time delay and the difference between the output of the process and the model (including time delay) is fed back. An ideal laminar flow system performance can be predicted and built into the predictor. An example of using the simple Smith Predictor scheme to the model from Figure 20 is shown in Figure 21. Controller response with the Smith Predictor is more rapid than in the case of using a PID controller only [Figure 22].

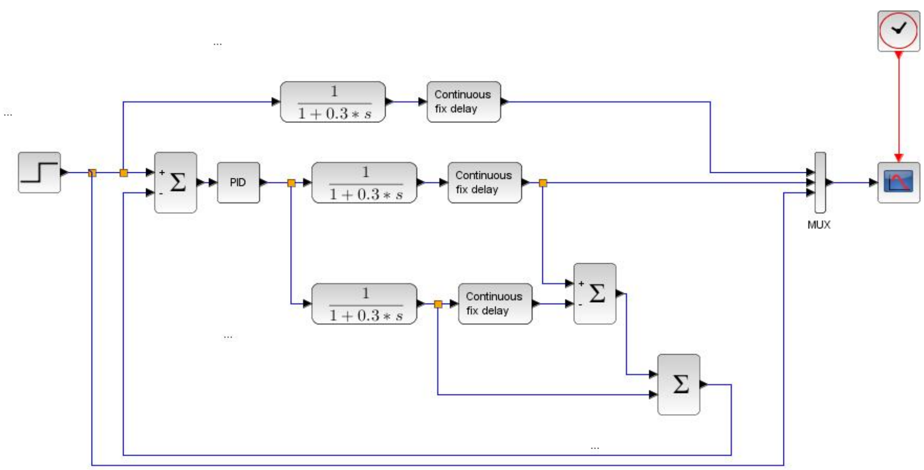

Figure 21. Scilab/Xcos diagram for a simple Smith Predictor scheme.

The previous case of reactor with a PID controller [Figure 20] may have the controller response time to reach the stable state shortened from 80 sec to about 30-40 sec. This example is a simplified model of the tubular flow reactor with ideal laminar flow velocity profile and is provided for illustration only. More advanced versions of the Smith Predictor control schemes are available [Sourdille and O'Dwyer, 2003; Normey-Rico, Camacho, 2007, 2008, Saravanakumar et al., 2007, Padhan and Majhi, 2011, Tasdelen and Ozbay, 2013].

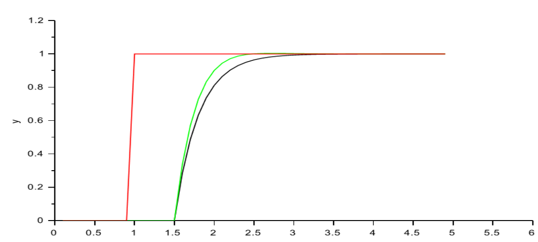

Figure 22. System and controller responses using the Smith Predictor (black - system response; green - response with the Smith Predictor).

The Smith Predictor controller may perform better than the PI controller at longer delay times. It may, however, develop stability problems at high gains. Instability may also occur if the real time delay is less than the model time delay. Adam et al. [2000] investigated stability of the Smith Predictor with uncertain delay times. They reported results using only the P controller type with proportional gain = 4. Veeramachaneni and Watkins [2014] proposed a design method for robust stable PID controllers using the Smith Predictor. They compared the PID standard controller with the Smith Predictor controller. Using the Smith Predictor increased the robust performance area of the PID controller. While many publications describe simulations using the Smith Predictor controllers and report computational results, practical approaches can be valuable to control practitioners. Veronesi [2003] reported on using the Yokogawa controllers for the Smith Predictor applications. He proposed a method of automatic computation of dead time for the Smith Predictor performance improvement. Normey-Rico et al. [2014] presented an automated tuning methodology for a dead time compensator. A modified (filtered) Smith Predictor control scheme was used. Simulations were compared with the experiments in a pilot plant. Tuning procedure used data from a closed loop plant operation. This tuning methodology can be used with stable, integral and unstable processes.

Other possible approach to control processes with time delay can be an Internal Model Control [Datta, 1998; Isidori et al., 2003; Chen et al., 2008]. In the Internal Model Control a mismatch in gain may have more significant consequences than a mismatch in time constant. Abe and Yamanaka [2003] compared the Smith Predictor control and the Internal Model control. The authors pointed out the importance of correct identification of the plant model. Book by Normey-Rico and Camacho [2007] may be a good starting point for design of controls for systems with time delay. It covers the Smith Predictor and other dead time compensators, as well as the model predictive control. Controller tuning methods are also presented in this book.

Figure 18 shows an example of a radiation/convection spray dryer with a proposed control concept. Liquid and gas flow are controlled locally. Three temperature zones inside the reactor are maintained at preset temperatures. Additional control loops can be introduced to this basic scheme, for example, gas outlet temperature may be used to control the liquid feed rate. Typical systems produce particles that are removed from the carrier gas in a solids separator. Condenser and gas-liquid separator may be optional unless the carrier gas is returned to the system after removal of condensate (closed system operation).

Reactor/dryer body can be positioned horizontally or vertically with downward or upward flow. Natural convection effects at the heater surface may act co-currently or counter-currently to the main gas flow. Computational fluid dynamics has been used in recent years to estimate the combined effects of laminar flow and natural convection in the systems with heat transfer from duct wall to flowing fluid. Shrivastava et al. (2009) reported on disturbances caused by the thermal convection effects in vertical and horizontal reactor configurations. Wasmund et al. (2007) modeled an aerosol reactor for optimizing product properties. Vertical tube configurations were investigated with the carrier gas flow directions upwards and downwards. Reactor model has been developed with an aid of computational fluid dynamics. Velocity profiles inside the tube were significantly different for the upward and downward flows. Effects of natural convection at heated wall could make the upward flow to closer resemble a plug flow reactor – an almost flat velocity profile could be obtained under certain conditions of gas flow rate and wall temperature. Such effects may diminish under reduced gravity conditions. A step disturbance in the inlet can be a change in the carrier gas temperature, or a change in liquid feed rate, or a change in solute concentration in liquid. These disturbances can affect outlet temperatures of carrier gas and particles. A wall temperature of the reactor can be controlled to remain at a predetermined level.

Performance of tubular reactor in real time may not be known without taking product samples. Wasmund and Coley [2009] investigated performance of the aerosol tube reactor including taking particle samples along the reactor length. Examination of samples led to changing reactor operating parameters to optimize powder properties. However, such research approach may not be feasible to be used in process control scheme of the operating reactor.

Kalani and Christofides (2000) have proposed a control approach to the aerosol reactor for production of titanium dioxide. The approach involved manipulation of the reactor surface temperature to obtain product with certain properties and size distribution. However, a practical implementation of the tubular furnace wall temperature adjustment for real-time control purposes may be a challenge due to relatively short residence time of products inside the reactor, and significant thermal inertia of the furnace. Typically, the reactor thermal operation is in a steady state. In some processes, multi-zone tubular furnaces are used with a certain wall temperature profile maintained along the tube.

G.3. Operation and control of dryers – possible approaches and selected details

G.3.1. Convection dryer

Highly automated systems may be desirable to reduce work burden on the crew. Typical controls of the spray dryer may be employed, e.g. using such parameters as inlet and outlet air temperatures, varying pressures along the system, power input to the heater, air flow rate and feed flow rate. In addition, humidity sensors may provide information for automatic performance monitoring and adjustment/optimization. Some additional temperature measurement points may be considered, such as air inlet/outlet in the energy recovery heat exchanger. If a condensing heat exchanger is used, its performance needs to be constantly monitored (inlet and outlet air temperatures, cooling agent parameters, and coolant flow rate). Confirmation of its performance can be the volume of collected condensate.

Brine concentration and composition may vary from batch to batch. Spray drying process operation may be mostly concerned about the solids content and composition in the brine, since they affects amount of water to be evaporated. Surface tension and viscosity may affect droplet size, in essence the evaporation surface of generated droplets. Performance of the particle collector should also be monitored. For filters, a pressure drop across the filter needs to be monitored.

Model-based control systems should have certain robustness and flexibility built in, to accommodate liquid properties changes that may occur from batch to batch. Such variability might be broader for brines than for products processed in the industrial dryers, which are better defined and follow tight specifications and therefore, a model once established, may continue to deliver predictable results. The model may be developed with an aid of process and system identification techniques [Keesman, 2011; Ljung, 1999]. Potential process disturbances, excluding hardware problems, could be as follows: change of composition of processed liquid, precipitation of solids in processed liquid, change of solids concentration in processed liquid, change in viscosity and surface tension of processed liquid, change in liquid temperature, change in air humidity (if an open system is used), change in flow rate of processed liquid, presence of gas bubbles in processed liquid, change in cooling temperature of condensing heat exchanger, change in moisture content of dried particles, change in size of dried particles, varying level of solutes in condensate, or particle separator performance degradation.

Some of these changing variables may depend on changes of other variables, for example, a change in dried particle size may depend on change in feed liquid viscosity and surface tension that lead to smaller droplets. Smaller particles may affect particle separator efficiency and some finer particles may enter condensing heat exchanger, fouling energy recovery heat exchanger and condensing heat exchanger and possibly dissolving in condensate, thus changing its composition and changing the load on the condensate/water purification system. If there is a filter after the main particle separator, more fines may increase load on this filter and its resistance to flow may increase. This may affect blower performance – air flow rate may decrease. Air heater would also be affected since air temperature may increase if air flow decreases. Depending on system instrumentation and controls configurations such disturbances can be countered by action of the control system, for example, the mentioned decrease in air flow rate may be measured by air flowmeter and countered by increase in blower rotational speed, or power to air heater may be decreased. Since the drying agent is air/gas, air flowmeter performance is crucial for system monitoring and control. Orifice or nozzle flowmeters may generate pressure drop and this may not be desirable if blower power minimizing is required. Ultrasonic flowmeter may not generate flow resistance and its accuracy may be adequate. Flowmeter location on the duct is critical – it has to be at a certain distance from flow disturbances such as elbows or dampers. Ruppel and Peters [2004] investigated effects of upstream disturbances on readings of an ultrasonic flowmeter. Flow disturbances were created by single or double pipe elbows. For the single elbow error has stabilized at about 1% at distances larger than 10x of the pipe diameter. The double elbow configuration flow disturbance may require longer straight pipe run – 20x of the pipe diameter or more. A flow straightener (for example, the Akashi type) may be used to improve flowmeter readings.

In industrial dryers air heater can use steam or electricity and it is usually locally controlled using an air temperature controller. In small systems air heater is electrically powered. The disturbances could be external, such as an air flow rate change, or may develop internally, for example, supply voltage to heater may fluctuate. Local air temperature control at such electric heater may have a short time delay if temperature sensor is placed close to the heater and the heater is of a heated wire type. The time constant of such heater may be short in the range of 5-15 sec depending on design and size. Electric heaters using sheath or sheath with fins may have longer time constants in response to voltage change. Ceramic heaters may have even longer time constants.

Not all of these changes/disturbances may be of significance, but one should consider how the composition and properties of brine might change and design the process and system to provide robust performance within certain boundaries. For example, system can be challenged by a sudden change in solutes concentration (a step change, for example from ending one tank of brine and switching to another). If concentration of solutes suddenly decreases then the amount of water to evaporate increases and moisture content in dried particles may increase changing their properties. Also outlet air temperature from the dryer may decrease and air relative humidity may increase.

Some changes/disturbances may occur rapidly (like a change in brine composition and properties), others may occur more slowly (like an increase in filter resistance). In design of controls one may focus first on system dynamic response to sudden changes and then evaluate slower disturbances. Slow changes may be well coped with by the control system, but they may lead to some undesirable permanent process deviations, therefore, process monitoring and alarms system should alert operators when such deviations do occur. An example can be an increase in filter resistance that leads to control system adjustment (an increase) in a blower rotational speed resulting in increase of blower power consumption, as well as increasing pressure in the system prior to the filter.

Frequently used control scheme is based on varying liquid delivery rate depending on temperature of air that exits the dryer. In the case of two-fluid spray nozzle or ultrasonic spray nozzle, these nozzles can accept varying liquid delivery rate without need of being adjusted internally themselves. Therefore, the controlling element is a feed pump that delivers liquid to the droplet generator. Small systems often use a peristaltic pump that by principle is a positive displacement pump and feed rate depends on pump rotational speed if there are no significant changes in backpressure the pump is pumping against. Both nozzles may provide relatively stable backpressure levels, thus one may consider that pump flow rate depends on a rotational speed. Peristaltic pump produces pulsating flow and the pump head design should be such to provide a minimal pulsation. Jorgensen and Lambert [2008] presented a brief review of peristaltic pumps used for biopharmaceutical dispensing. A “pulsation-free” pump was described (the Flexicon). Reduction of pulsation is achieved by using a double tube head with offset multiple rollers. Pump accuracy over a long period of time may be $\pm$ 0.5%, or better. Peristaltic dispensing pumps are designed to run at high rotational speed to minimize fill time, and are equipped with a control system that provides an immediate response from the filling machine input signal. Pump dynamics depends on its controls and on a motor type and pumping head drive that is used. Tubing properties can affect pump dynamics as well. Pump manufacturer manual may not contain data on pump dynamics, therefore users may need to conduct pump dynamic response test. The pump may operate in an open control loop, e.g. the pump rotational speed is changed as a part of control of dryer outlet air temperature. The pump may also have a more advanced feedback closed loop with a flowmeter between the pump and the droplet generator.

Ortega-Palacios et al. [2010] investigated a transit time ultrasonic flowmeter working in combination with a peristaltic pump. Flowmeter followed closely the pump pulsations. Similar systems are used for pumping blood during surgery, e.g. when pulsations are required. Ultrasonic flowmeter has been found adequate for such application, thus it should provide satisfactory performance with dampened pulsations as well. Yao et al. [2004] combined two ultrasonic techniques in an ultrasonic flowmeter: the transit method with the Doppler method. Accuracies better than $\pm$ 1% were obtained for flow velocities larger than 0.8 m/sec. Location of such ultrasonic flowmeter should be on a straight line since turbulence may affect readings. Flowmeter should be installed at least 20x of the pipe diameters from the disturbance [Sanderson, Yeung, 2002]. If its location is 5-10x of the pipe diameters from the disturbance point, a negative reading error can occur within the 5-12 % range. Higher measurement accuracy could be obtained using a mass flowmeter based on the Coriolis effect. Accuracy of the meter can be $\pm$ 0.1-0.15%. For example, Emerson/Micro Motion company [Emerson company literature, 2014] offers the Coriolis flowmeter line for low flow rates that may be comparable to requirements for small spray dryer design. The LF3M model has maximum liquid flow rate 1.0 kg/hr for liquid and 0.405 kg/hr for gas. For the model LF4M these numbers are 27 kg/hr and 3.64 kg/hr, respectively. Mass flow accuracy is $\pm$ 0.50%. This meter can also measure density of the fluid. Density accuracy is $\pm$ 0.005 g/cm^3.

The control system may include flowmeters on the liquid feed line and on the air supply line. Flowmeters themselves are components with a certain dynamic response and they may affect overall system dynamics. Manufacturer literature may not provide flowmeter dynamic characteristics. Wiklund and Peluso [2003] provided data on dynamic responses of various types of flowmeters, including transfer functions. The flowmeters listed were based on pressure difference transmitters, vortex pulsation, magnetic coil, and the Coriolis principles. The tested liquid was water. In general, the fastest response was provided by the pressure difference-based flowmeters.

If a humidity sensor is a part of the control scheme its selection should include temperature range, humidity range and accuracy. Typical accuracy may be $\pm$ 0.8 – 1.0% RH. Humidity sensors may have relatively long time constants in the order of 8-20 seconds. Sensor performance needs to be combined with a temperature sensor with time constant of about 1-2 seconds. The dryer control system may respond to the temperature change first and then further adjust according to a relative humidity reading. For example, adjusting feed flow rate down, if temperature of outlet air decreases, and then adjusting it again after stabilized reading from a humidity sensor is obtained. A safe operational goal may be a low moisture content of powder with outlet air relative humidity being also low, and outlet air temperature correspondingly high. There may be no need to get as low as possible outlet air temperature regarding dryer thermal efficiency, if a gas-to-gas energy recovery heat exchanger is employed. Outlet air temperature limits may be affected by liquid and particle properties related to thermal degradation.

If brines are prepared from hygiene and washing water, then there may be surges in surfactants present in brine resulting in significant changes in surface tension. This may not only change droplet diameter, but also change droplet drying process if surfactants forms a layer on droplet surface. A system challenge test could be a step increase in surfactant concentration from a typical to the worst anticipated case.

G.3.2. Radiation/convection drying

Convection-radiation dryer control and automation concept may require more development work. Typically, aerosol flow reactors do not work in a mode of recovering solvent or water. The target is a quality of particles produced, and this may include particles size, possible agglomeration, chemical reaction completeness and solvent or water content. In the case of water recovery, dryness of produced particles may be related to amount of evaporated water and particle temperature history may be related to particle degradation, including chemical reaction and production of undesirable by-products.

Slow or delayed responses are expected regarding radiant heating and aerosol flow. For example, radiant heating may be based on voltage change to the electric heater, pulsing the heater power supply on/off, or using signals from temperature or infrared radiation sensors. In most radiant heating applications, a thermocouple is used to sense heater temperature, and this temperature is controlled. Operating temperature of the heaters is typically higher than the processed product temperature. Such control may be combined with the use of an infrared sensor that senses infrared radiation emitted by the heater, or by processed product, in this case radiation emitted by dried particles.

Advanced control concepts may be employed since this can be a process with a significant time delay. Examples of control concepts could be a feedforward with feedback scheme, a Smith Predictor, or a model-based control.

G.3.3. Control system interface

In the case of brine processing, spray drying system can be integrated with water recovery system and be a part of overall control scheme. For example, a display of water recovery system can have multiple layers with the top layer showing only information that everything performs well, displaying current water recovery rate. In the case of deviations or alert messages, display may be allowed to switch from that top layer display to a display that shows actual system with deviation, for example to a spray drying system display. Spray drying system interface with a human operator can have a graphic display with an image of the system with critical parameters displayed in real time, and in the case of deviations, these points should have clearly marked alarms with multiple severity levels. An intelligent system control could then display diagnostic windows overlays with suggested remedies and actions that may be taken by the operator. Multiple alert levels should be provided possibly up to system shutdown if the operator fails to take action. However, the operators may be occupied with other tasks and for this reason these multiple alert levels need to be stepped through before system shutdown. These alerts may be accompanied by actions taken automatically by intelligent control system to correct process performance – information about corrective action should be provided to the operators and recorded. An intelligent control system concept and its detailed design may assume that operator expertise can be limited. This is an example of possible approach to a research system controls with certain level of autonomy provided for the system, which performance is going to be tested in microgravity.

Actual operational space-bound system may have similar control concept, however it should be in-line and integrated with the spacecraft controls overall concept and protocols, communications and telemetry. Link to the space control experts should be available and data can be sent to the data center including routine performance, deviations, corrective actions, alerts and alarms, and operators actions. At certain conditions an alert and alarm levels request may be automatically send asking for the space center experts more direct involvement. These steps should precede system shutdown that may only occur after all corrective actions are taken.

Below is an example of the International Space Station controls interfacing with ground monitoring. In the International Space Station (ISS) Mission Control Center, teams of experienced flight controllers work at monitoring consoles. On the top of each console is the "call sign", an abbreviated name for the console. The name of the console position is based on the responsibilities of the flight controller. The flight controllers monitor crew's activities, health, and safety. They also monitor the spacecraft equipment and software. Water processing systems are included in the ETHOS Console [ETHOS Console Handbook, 2014]. Figure 23a shows an example of the ETHOS console overview display including water and urine processing.

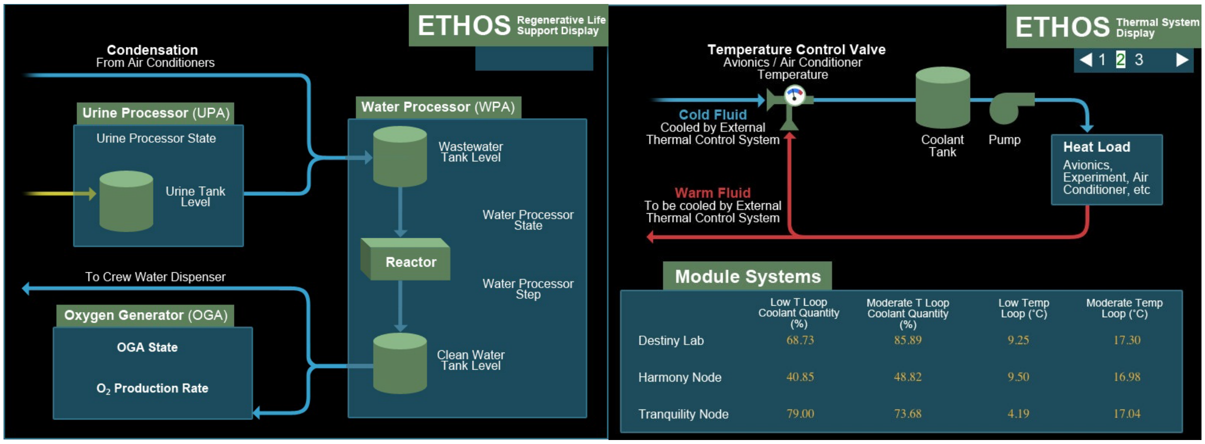

a) **b)**

Figure 23. Example of the International Space Station console display at the ETHOS systems level.

Figure 23b shows a Console display of the ETHOS Thermal System. The 12 active fields can display actual data continuously in real time – shown in yellow. Future spacecraft systems may take a similar, or a modified or completely new approach. For long duration, long distance missions, for example, the Mission to Mars, real time monitoring and control input may not be possible because of communication time delays and more autonomous control systems may be required.

H. Energy management

H.1. Convection-based dryers

Energy efficiency of a space-bound spray dryer will be an important factor. Industrial and research convective spray dryers are known to possess relatively low thermal efficiency and steps such as an increase of the gas inlet-outlet temperature difference, and an increase in concentration of liquid feed are typically used to improve dryer efficiency.

In a simple system configuration, ambient air is drawn from the environment, filtered and passed through a heater and then it enters the drying chamber. Exhausted air may pass through a particle separation device and a filter and is discharged back to the environment. Thermal efficiency E of the spray dryer can be described as ratio of the heat used in evaporation to the heat input [Masters, 1991]:

$E = (T_1 – T_2)/(T_1 – T_0)$; where: T_1 is air inlet temperature; T_2 is air outlet temperature; T_0 is temperature of ambient air that is drawn into the dryer. For example: If ambient air temperature is 20 C, and air inlet temperature is 135 C and air outlet temperature is 85 C, then overall thermal efficiency is 43.5%.

Thermal efficiency can be improved by using high inlet air temperature while maintaining low air outlet temperature. If inlet air temperature is 200 C and outlet temperature is 90 C, thermal efficiency will be 60%. However, if an increase in inlet air temperature is followed by an increase in outlet air temperature, efficiency may not increase and could even decrease. Kajiyama and Park [2010] investigated effects of inlet air temperature and relative humidity of ambient air on energy consumption and on dryer efficiency. Air inlet temperatures were between 100 C and 140 C and ambient air humidity was between 20% and 80%. Increasing inlet air temperature and relative humidity of ambient air led to decrease in dryer thermal efficiency. However, such system is not very energy efficient in general, since exhaust air temperature is higher than ambient air temperature.

An air-to-air heat exchanger can be used to improve dryer energy efficiency. An exhaust air can transfer its energy to incoming ambient air. At inlet air temperature 135 C if air-to-air heat exchanger preheats air to 60 C and cools dryer outlet air from 85 C to 45 C, overall thermal efficiency may approach 78%. Performance of air-to-air heat exchanger may depend on quality of particle separation upstream from it since dust may accumulate on heat transfer surfaces. Industrial heat exchangers may have liquid cleaning systems to periodically clean heat transfer surfaces. There may be no condensation involved in operation of such air-to-air heat exchanger. In the case of using an efficient heat exchanger some condensation may occur and exchanger design should provide for condensate removal. In the case when water or solvent recovery is required, an additional condensing heat exchanger/condenser can be applied in exhaust air path after the air-to-air heat exchanger. Such condensing heat exchanger requires additional cooling – it can be air cooling using ambient air, or using other cooling resource (examples: a chilled liquid, a thermoelectric cooler) to be able to operate independently from the ambient air temperature. Using the air-to-air heat exchanger cools exhaust air prior to condensing heat exchanger and thus reduces cooling requirement for this exchanger. Discharged air has reduced water content.

In the cases of using solvents different than water, closed loop drying systems have been used often employing an inert gas such as nitrogen. Use of a closed loop system may also be recommended in the case of water, if the drying product releases any compounds that cannot be directly vented into atmosphere. Figure 24 shows a closed loop spray drying system configuration.

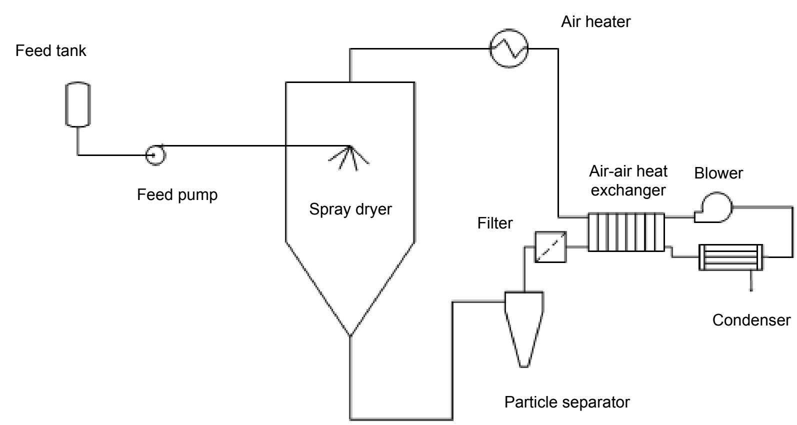

Figure 24. Closed loop spray dryer with energy recovery and solvent/water recovery.

In the cases of using organic solvents, condensing heat exchanger is used for solvent recovery. A similar principle can be employed for recovery of water. If solvent or water purity is an issue, then further liquid purification steps may be employed after the condensing heat exchanger. This may become an important issue if dried product releases some undesirable compounds that may end up in condensate. Purity of the condensate may depend on quality of particles and fines separation, e.g. no fines should contact with and dissolve in condensate, and on the presence of gaseous compounds formed during drying that can dissolve in condensate.

System can operate in an open loop configuration if the air quality after condensing heat exchanger meets the current air quality standards, thus allowing air discharge to the cabin. In such case, the blower air intake will be directly from the cabin. Current version of the Spacecraft Maximum Allowable Concentrations for Selected Airborne Contaminants (SMACs) document should be consulted to decide on open or closed air loop configuration. Advantage of the closed loop configuration can be the independence from ambient air humidity and temperature since these parameters can be controlled by operation of the condensing heat exchanger.

An absorber/scrubber may be installed prior to the condensing heat exchanger to remove traces of fine particles and gaseous compounds that may dissolve in the condensate. Such a step may improve condensate purity, yet the absorber would require cleaning or replacement of its liquid phase that traps fine particles and gases. Absorber may also remove contaminants that may not dissolve in condensate and exit with air – improving the air quality may allow venting it to the cabin. Optional location of absorber can be after condensing heat exchanger if absorber needs to purify air vented to the cabin and condensate impurities can be managed by water purification system. Current Spacecraft Maximum Allowable Concentrations for Selected Airborne Contaminants (SMACs) document should be applied as well.

Design and operation of gas-to-gas heat recovery exchangers, condensing heat exchangers and gas absorbers were described in the report by Wisniewski [2014]. Preheating of liquid may further improve system energy management. Liquid preheating prior to spraying may affect the atomization process and flash boiling phenomena may occur [Sher et al., 2008]. Heat recovery from dried powder is typically not used.

H.2. Radiation-convection spray drying systems

In a radiation-convection drying system, heat capacity of carrier air is far lower than in convection drying systems, but can be higher than in a radiation-based system with very limited air flow.

Carrier air can reach high temperature near water saturation level since most of the energy is provided by radiation. Therefore, if an air-to-air heat exchanger is employed to preheat incoming carrier air, condensation may occur inside this heat exchanger on the exhaust air stream side. With a small amount of carrier gas, the gas stream heating and cooling steps would involve less heat transfer than water condensation and therefore, the gas-to-gas heat exchanger may not be needed. Condensation step can be accomplished in a condensing heat exchanger as in the case of convective dryers.

The dryer needs to be thermally insulated so there is a minimal heat loss to the environment from its external walls. Almost all energy delivered by the heater would be utilized for water removal in evaporation and drying of droplets.

I. Cleanability

Small laboratory systems may be cleaned in cleaning stations after disassembly and if needed, their components may be autoclaved. Figure 2 shows an example of a pharmaceutical grade laboratory spray dryer, designed for easy cleaning. Industrial spray drying systems use automated cleaning, so called Cleaning-in-Place (CIP) method. Large systems have arrays of spraying nozzles distributed into multiple piping circuits to clean the system sequentially. A dedicated cleaning station is used to prepare the cleaning and rinsing solutions and pump them through the nozzles to clean the system internally. The cleaning station includes solution preparation tanks, a piping system with array of valves and pumps, and a control system that monitors the properties of cleaning and rinsing solutions to ensure that cleaning is sufficient. The CIP approach to spray drying was summarized in a GEA Niro technical brochure [GEA Niro company literature, 2012]. General principles of CIP technology were described by Seiberling [2008]. The CIP process covers the drying chamber, separation cyclones, ducting after the drying chamber, heat recovery heat exchangers and even the bag filtration systems. Cleaning is done by spray impact and by liquid film flowing on the cleaned surface. Surface cleaning quality is tested and validated. Cleaning liquids are delivered at elevated temperature. In small laboratory systems, there may be no need for the CIP process of this kind since the systems may be cleaned manually, or filled with cleaning and rinsing solutions that are circulated throughout the system. The circulation rate may generate high local stream velocities and turbulence that will aid in contaminants removal. Properties of cleaning solutions may be monitored. In large systems, use of CIP is dictated by the need to minimize volumes of cleaning and rinsing solutions. This could also be a concern for smaller systems if there is a problem with cleaning solution disposal. A consideration could be given to a hybrid approach: the system components with larger volumes (example: drying chamber) being cleaned by spraying, and components with smaller volumes (examples: ducting, particle separator) by flooding with liquid circulation. Solution preparation and cleaning processes can be automated. The cleaning-in-place step can be followed by sanitization-in-place or sterilization-in-place. Due to the size of spray dryers, this is accomplished by chemical means, not by clean steam. Liquids or vapors can be used in this step. For example, the hydrogen peroxide vapor is often used for sterilization of equipment in pharmaceutical industry [Sandle, 2013]. In-situ generated hydrogen peroxide may be also used for biological inactivation, disinfection and preservation steps. An electrochemical generation of hydrogen peroxide may be employed when small quantities are needed [Qiang et al., 2002].

J. Microgravity and reduced gravity operation

Convection and radiation/convection spray dryers may benefit from reduced gravity or microgravity. The droplet free fall phenomenon may be reduced or eliminated, therefore, the droplet residence time in the dryer can be controlled by flow of a drying gas or a carrier gas. The natural convection effects at the heated wall may disappear and thus the stream velocity profile may remain undisturbed. The droplets can be made larger and the residence time longer if larger particles are required for easier separation from the gas stream in both, convection dryers and dryers/aerosol flow reactors.

J.1. Product properties

Typically the spray drying product of interest are dried particles and sometimes it is a recovered solvent. Dried particles' properties are always of importance since they should not degrade or decompose. Even if the particles are not of primary interest, the products of their decomposition should not contaminate the drying or carrier gas stream or the recovered solvent or water.

Particles should not be sticky, since that they could permanently attach to the components and walls of the equipment, clog the ducting, or hinder the performance of particle separation equipment. In large spray dryers, air flow pattern and particle trajectories may be configured to reduce contact between particles and the wall. Yet the particles still can land on the wall of the bottom cone. The general approach to particle motion in the boundary layer and their deposition on the wall [Rogers, Eaton, 1991; Chhabra, De Kee, 1992; Taniere et al. 1997; Gharraei et al. 2007] may have limited use since the particle motion and deposition may also depend on gas flow pattern in the spray dryer. Guha [2008] reviewed transport and deposition of particles in turbulent and laminar flow and presented multiple mechanisms of particle deposition. Aydin et al [2014] proposed a CFD model for gas-solid suspension flow near the walls including a rebound effect. Keshani et al. [2015] reviewed the general subject of particle wall deposition in spray drying processing.

Sticky particles are sometimes produced in the food industry and various measures have been employed to reduce particle stickiness or reduce particle adhesion to surfaces. Particles temperature and air outlet humidity can be controlled, or/and additives can be mixed with the liquid and the resulting particles may become less sticky. The equipment surfaces can be kept under controlled temperature, or/and can be modified to reduce particles stickiness [Adhikari et al., 2005; O'Callaghan, Hogan, 2013; Woo et al., 2009]. Cooling of dryers' wall, or using a cold air sweep along the wall are sometimes applied to lower particles temperature below the glass transition point.

Dryer walls can be coated to reduce particle sticking. Coating may be selected depending on the range of brines to be processed in the dryer. As a first step, anti-sticking PTFE or ceramic coatings may be considered. Surfaces inside the spray dryer and particle collector can be modified to reduce or eliminate particle adhesion. It has been known that the low energy surfaces may reduce degree of sticking. Considered surface materials and coatings need to have their surface energy determined [Zenkiewicz, 2007]. Surface energy can be manipulated to reduce formation of the particle-wall liquid bridges [Woo et al., 2009]. This can be applicable for "rubbery" particle-wall contacts at relatively low wall temperatures when particle temperature is not beyond its glass transition temperature. Lower wall surface energy does reduce the deposition of amorphous particles. This can be even more pronounced for deposition of droplets. Drummond and Chan [1996] analyzed "nonstick" materials regarding their free surface energy. They concluded that surface free energies can be a good guide to the relative adhesive behavior for low surface free energy ("nonstick") materials, such as fluorocarbon, silicone, and hydrocarbon solids toward the organic "soils" when the interactions are governed by the van der Waals (dispersion) forces. Theoretical considerations suggested that the fluorocarbons are the best candidates for ultra-low-adhesive materials, and no smooth homogeneous organic solid can be strictly "nonstick" toward organic "soils" in water.

Further research can be conducted on deposition of brine droplets and dried particles on surfaces with various surface energy, including surface coatings. Research may also include surface modifications of electrostatic precipitator electrodes. Past research of spray dryer surfaces has been mostly related to food and pharmaceutical products and since the brines involved can be unique, additional laboratory research work will be required. Surface hydrophobicity may not be the only characteristic required – it may well interact with the droplets and partly dried particles, but may not be effective for sticky dried particles with other than water liquid components.

J.2. Development and experimental work

While a ballpark performance of convection spray dryers may be estimated in advance due to relatively well-characterized spray drying process and large volume of data available for broad variety of products, an experimental work is always conducted during spray drying process development. Droplet and particle size affect not only the drying process, but also particle separation and powder handling. A small scale spray dryer may require smaller droplet size than a large spray dryer.

Drying fine droplets in aerosol flow reactors requires a more thorough investigation and more experimental work due to limited data that may be applicable to the process of interest. Droplet diameter is smaller and individual droplet evaporation can be shorter with the particle separation step influenced by low gas flow rate and fine particle size.

A preliminary research on droplet drying conditions can be conducted using a single drop drying technique. Droplet can be suspended on a fiber or needle [Fu et al., 2012], or be levitated using ultrasonic levitator [Bjelobrk et al.; 2012, Brandt, 2001; Yarin et al., 1998]. An example of a spray drying process development approach can be a set of procedures combined into the Drynetics method by GEA Niro company [GEA Niro company literature]. It consists of 3 major steps: single droplet experiments, advanced data analysis and CFD simulations. Single droplet experiments are conducted using acoustic levitation and they include temperature history, change in droplet size, droplet and particle stickiness and particle morphology. Subsequent advanced data analysis is based on these droplet experiments. It includes drying kinetics, particle moisture content change and particle density. These steps may also be followed by a laboratory scale spray drying test. CFD simulations involve velocities and particle trajectories in the drying chamber, temperature distribution in the chamber, particle moisture levels and air humidity. Simulations also involve estimates on formation of particle deposits on the chamber walls. For spray drying CFD simulations GEA Niro uses a supercomputer that contains 512 cores, has 90 TB of disk space and 2 TB of RAM. These investigations can provide background for conducting pilot plant experiments. The Drynetic method is backed by a vast database using practical experience - GEA Niro company has been building the spray drying plants for decades with the number of industrial installations in the range of tens of thousands.

Experiments with single droplets may not translate directly to drying of the liquid spray since drying conditions change within the spray and there may be also droplet-droplet interactions. Different combinations of spray patterns and drying gas flow patterns may produce different results. For example, a conical spray pattern from a high pressure nozzle may produce different drying conditions for the hollow cone and the solid cone sprays – the hollow cone can produce more uniform drying conditions for most droplets than the solid cone. Additional parameters can be involved such as hollow cone angle, cone layer thickness and configuration of drying gas stream contacting the spray cone. Large spray dryers may have gas distributors that surround the spray and produce gas jet that contact the spray under certain angle. Such gas jets can be straight or swirled. In small dryers a typical gas pattern is a streamlined flow parallel to the drying chamber side walls.

Dehydration of droplets can be more homogeneous if the liquid atomizing device can produce droplets of equal size. In practice, one should apply atomizing devices, which can produce sprays with narrow size distribution spectrum. In general, liquid atomizing devices that are used in small spray dryers produce smaller droplets with narrower size distribution than atomizing devices used in large dryers.

J.3. Water recovery

There may be options regarding condensing water from the dryer outlet air stream:

a)Venting the spray dryer exhaust air back into the cabin without water condensation and with the spacecraft atmosphere revitalization condensing heat exchangers condensing moisture from the spray dryer outlet air stream after it is mixed with the cabin atmosphere.

b)Venting the dryer exhaust air back to the cabin after passing the air through the dryer's own condensing heat exchanger and exhausting the dehumidified air back to the cabin.

c)Running the spray dryer in a closed loop. The loop includes a condensing heat exchanger for water removal from the recirculating air. The dryer exhaust air may not get mixed with the spacecraft cabin atmosphere. Such isolation may be beneficial if there are traces of volatiles from the brine in the dryer outlet air.

The cases b) and c) require a dedicated condensing heat exchanger working as a part of the spray dryer system.

All three cases can use a heat recovery gas-to-gas heat exchanger to recover energy from the dryer outlet air and preheat the drying air prior to air heater. This will be important for energy savings for air heater, but also in the cases a) and b) air returned to the cabin may be thermally more acceptable: in the case a) it will be cooled by incoming drying air, which is drawn from the cabin and in the case b) the cooling requirements for condensing heat exchanger will be reduced.

Condensing heat exchanger design may follow established designs of space condensing heat exchangers with some adaptation work to match the scale of spray dryer and to optimize system performance.

J.4. Particle separation

Microgravity environment poses a significant challenge to separation and handling of fine particles, including safety concerns.

Type of dryer may impose different conditions upon working principle and performance of particle separator. Convection spray dryers require separators that can not only handle the particle load, but also the high gas flow rate. High gas velocity may be utilized to assist separation process, as it occurs in the cyclone devices. Typical cyclones work in a vertical position with particles discharged from the bottom cone into the hopper. There are commercial horizontal cyclones and they also have particle discharge to the hopper that is assisted by gravity [Aerodyne Corp. literature]. One may utilize the rotating flow as means of particles ejection into a particle trap zone – such approach may be considered for microgravity applications, but a development work is needed. Axial flow cyclone designs may serve as a foundation of such development work. Axial flow cyclones from Kirk company [Kirk Process Solutions company literature] can work in a horizontal or vertical position. Part of the discharge flow can be recirculated into the inlet stream. Radiation-convection dryers may experience a low gas flow rate, thus their particle separator should be designed for particle load using separation that is not assisted by gas velocity. Solids produced by spray drying of brine may be not the product but waste and this is opposite to the commercial spray dryers applications.

Other possible particle separation devices could be based on the electrostatic forces and then the particle removal device may need to be designed to collect the particles from the electrodes. For the dry particles it could be a mechanized brush. For the sticky particles it can be a scraper. The brush can be in a roller form. These can be disposable pieces and could be coated with adhesive, or electrostatically charged to positively collect particles from the surface without stirring them up into the containing volume. This is, however a more complicated and uncertain approach than filter bag consideration. Bag type filter collectors may offer containment of the powder and may allow developing safe bag removal and disposal procedures. Filter for a convection dryer may be sized considering the air flow and particle load. Filter for a convection-radiation dryer can be sized to match the particle load.

In general, in many types of particle-gas separators, the separation process may be gravity-independent yet the collected particle discharge and handling may depend on gravity. In the case of cyclones, particles fall into the hopper located at the bottom of the cyclone. In the case of the bag filter, the particles are periodically removed from the bag by the cleaning device and fall into the hopper below. Also in the case of the electrostatic precipitators the particles are either dropped from the electrode surface or carried down by a liquid film. At relatively low particle loads, filtration devices may be employed. Filtration has been broadly used in the processing of aerosols [Ruzer, Harley, 2013]. To facilitate powder handling these devices can be made disposable. This would impose a condition of small volume and low mass for the filters. Filters can be made in form of a bag that can be compressed after use with the dust inside. Electrostatic precipitator may have a removable dust-collecting electrode that may be disposed with the dust. Typical dust-collecting electrodes are made of metal, thus disposable electrodes could possess substantial mass and they may be too large to supply and manage after use. A disposable electrode might be made of metalized polymers, or of conducting polymers and collapsed and compressed after use with the powder enclosed.

J.5. Design and construction

Laboratory spray dryers are typically built of glass to satisfy laboratory standards, as well as to allow visual observation of the process, including the spray, droplet evaporation and particle formation, and to identify potential problems with product stickiness and the areas where product may stick. Glass construction and sanitary type seals permit easy cleaning of the dryer when changing from product to product. Space bound spray dryer may be applied to one, or a few products, thus it can be designed to accommodate their characteristics. Design with glass components may be problematic and a metal design can be considered, but dryer may have windows built into its walls to allow visual inspection. Components may be made of metal and other materials and the walls may have a coating using low surface energy materials to minimize product sticking. The dryer design shown in Figure 2 demonstrates an example of stainless steel cleanable system construction.

If there is a system design requirement that the system takes air from the cabin and discharges it back there, then an energy recovery heat exchanger needs to be installed not only to save energy but also to reduce temperature of the outlet air. A condensing heat exchanger further cools air stream to recover water. Energy recovery heat exchanger can reduce cooling rate needed by condensing heat exchanger, as well as can reduce heat input to be delivered by the heater. If there is a system design requirement that the dryer has to operate in a closed loop, these heat exchangers can be employed as well.

Additional subsystems may, or may not be needed depending on results of tests of the dryer using considered brines. For example, exit air may require additional treatment. If necessary, particle separator may be followed by an adsorber to capture volatiles that are present in the air. This could be a double-walled bag similar to a bag filter with adsorbant placed in the bags. Eventually such device could play a dual role of a filter and adsorber.

If necessary, an absorber with circulating liquid may be used for treatment of the exit air. It may have a dual role of capturing traces of fine particles that passed the particle collector and also providing absorption with chemical reaction capability to absorb traces of volatiles and neutralize them. Such absorber could be based on a Venturi nozzle principle, or be a rotating packed bed, or a rotating surface thin film type.

J.6. Design guidelines for microgravity and reduced gravity spray dryer designs

Microgravity could be an ideal setting for a spray dryer that might require longer droplet drying times. Spray dryer design for microgravity may be based on terrestrial spray dryer designs, yet due to microgravity factor it might depart from typical design solutions and employ design features that can be uniquely specific for microgravity conditions.

Primary process factors in spray dryer design are: required evaporation capacity and product thermal stability. System design factors are: heat delivery concept for droplet evaporation, spraying system design and mean droplet size it can produce, drying temperature, droplet evaporation/particle formation times, droplet/particle stickiness, particle separator design principle and its separation efficiency, system overall efficiency and collected material discharge operation.

Other factors can be design and operation of condensing heat exchanger and choice of open or closed loop system. Use of a condensing heat exchanger facilitates design of the closed loop system.

Space applications may impose multiple constrains on system design and operation. Typically these are minimum mass, volume and power requirements. Other requirements can be reliability, simplicity of design and operation, and minimum maintenance and service. System should be also easy to fix after failure and requiring minimum crew effort to do this. System performance should be robust, insensitive to changing operational conditions (example: changes in brine quantity and composition). This includes a robust control scheme to be employed.

Research drying equipment can be tested in a parabolic flight since the fine droplets can be dried in short times comparable with periods of microgravity conditions that may be achieved.

J.7. Design concept for a space based spray dryer

J.7.1. Convection heat delivery

Spray dryer using hot air or gas with convection heat delivery for droplets evaporation seems to be the simplest path to system development due to large volume of available data for such type of dryers, including laboratory and research systems that are close in capacity to systems that may be needed for space applications. The key issues are: generation of very small droplets at uniform diameter, adequate droplet-drying gas contact and efficient particle separation. Two first issues allow rapid and uniform droplet drying and may lead to a compact dryer design. Particle separation system may require additional development work to be able to operate under reduced gravity or microgravity conditions.

J.7.2. Radiation heat delivery

Heater types could be a ceramic or carbon type to provide match between their radiation peaks and radiation absorption peak of water. Metallic wall heaters with special coatings may be developed. A slow controlled gas flow may be required to carry droplets and particles through the system thus introducing some convection effects. Existing droplet generators can produce very small droplets/aerosols. Particle separation system may require development work.

For a terrestrial test bed heaters should not provide significant natural convection effects since such effect may not be present in microgravity. Tests in parabolic flight may be required to eliminate effects of convection.

J.7.3. Mixed convection-radiation heat delivery

For thermally sensitive products where low intensity radiation may require large heater surface areas, a combination of radiation and convection may be used. Preheated gas will contact the spray and serve as a carry agent for droplets and particles, whereas radiant heaters can be located in the drying chamber providing heat input to gas-particle suspension. Radiant heat transfer should be controlled to prevent overheating of droplets and partly dried particles. Residence time of particles can be extended and the dimensions of the drying chamber could be reduced in comparison with convection dryers.

Typical laboratory aerosol flow reactor designs use cylindrical tube with heated walls. Under laminar flow conditions such reactors may dehydrate the droplets near the center last. One may consider adding a central cylindrical heater to create laminar flow in annulus, with the last droplet evaporation and drying to occur in a certain round zone along the radius. Since radiation surface area of external heater will be larger than central heater surface, such last drying zone may be located close to the central heater. Internal and external heaters will be independently controlled. Central heater should possess adequate radius to ensure meaningful radiation flux without need to operate this heater at high temperatures that may be detrimental to the product. Central heater may be of segmented design with individually controlled zones to provide certain surface temperature profile and different radiation fluxes along the heater. Existing droplet generators may produce very small droplets/aerosols. Particle separation system may require development work.

To reduce radiant heater surface temperature, air can be used for heater cooling and that preheated air can be then used for convection part of drying. This way the drying air heater power rating and size can be reduced. For aqueous brines the heater peak radiation wavelength of 3 micrometers may be considered.

Radiation-convection based dryer development can pose many challenges to reach optimal system design and performance. Further research and development projects may lead to small droplet drying systems that could improve performance of the existing commercial and laboratory equipment and be applied for terrestrial and space applications. More details on spray drying technology and systems can be found in the report by Wisniewski [2014].

III. Summary

Reduced gravity or microgravity conditions may provide advantage in droplet processing, since free fall of droplet under gravity may be reduced or eliminated and therefore, droplet size and residence time in the processing apparatus can be more flexible using flow of a drying gas or a carrier gas. Slower free fall velocity, or no fall velocity may allow reducing size of the processing apparatus. Reduced gravity or microgravity may also reduce, or eliminate effects of natural convection in laminar flow aerosol processing system. Microgravity environment would allow any position of the spray dryer due to absence of particle settling effect.

Current status of convection spray drying and aerosol drying systems can be used as background for system design for space applications, including reduced gravity and microgravity conditions. Convection-based spray dryers are more matured designs available commercially. Drying time is short and droplet and particle overheating may be avoided due to evaporative cooling that rapidly lowers processing temperature. Adaptation of convection spray drying systems to microgravity may require redesign or new development of particle separator.

Aerosol drying systems are used for laboratory work as well as in industries where drying of droplet can be primary (nanoparticle manufacturing), or secondary (coating, semiconductor manufacturing) goal.

Adaptation of aerosol drying systems to microgravity may also require development of particle separator, with such options like electrostatic precipitator and filter. Due to low carrier gas flow rate, filtration may be considered a main separation step.

Liquid atomization may be critical to system design and performance. Droplet size may affect the drying process, as well as selection and performance of particle separator. Droplet size distribution shall be very narrow. Droplet size may be affected by solutes present in the liquid.

Liquid pretreatment should involve a concentration step (for example evaporation) to reduce amount of water to be removed in the spray dryer. This would improve dryers' thermal efficiency and reduce system dimensions.

Design of auxiliary subsystems such as droplet generator liquid feeding, or water condensing/recovery should not pose significant challenges considering the current state of the art.

Attention should be paid to system automation including system dynamics and possible variability of feed solutions. Variability of feed solutions may impose additional challenge on model-based predictive control schemes. Measurement of key feed properties that affect spray drying process may be required to aid the models used in control and facilitate implementation of autonomous control systems.

In addition to the usual factors like system mass, volume and power requirement, also reliability and feasibility of system automation should be considered in technology selection and system design and operation.

References

Abdallah A. et al., Symmetric plate resonators for viscosity and density measurement, Procedia Eng., 87, 36-39, 2014.

Abe N., Yamanaka K. Smith Predictor control and Internal Model control, SICE Ann. Conf, Fukui, 1383-1387, Aug. 4-6, 2003.

Abraham J., Sparrow E., Tong J. Heat transfer in all pipe flow regimes: laminar, transitional/intermittent, and turbulent. Intl J. Heat Mass Transfer, 52, 557-563, 2009.

Adam E., Latchman H., Crisalle O. Robustness of the Smith Predictor with respect to uncertainty in the time delay parameter, Proc. Amer. Control Conf., 1452-1457, Chicago, June 2000.

Adhikari B., Howes T., Lecomte D., Bhandari B., A glass transition temperature approach for the prediction of the surface stickiness of a drying droplet during spray drying, Powder Technol., 149, 168-179, 2005.

Adiga K., Willauer H., Williams F. Droplet breakup energies and formation of ultra-fine mist, Naval Research Laboratory, Washington, 2007.

Aerodyne Corporation, company literature, Chagrin Falls, OH.

Alvarez M., Friend J., Yeo L., Arifin D. Microaerosol and nanoparticle synthesis for drug delivery via surface acoustic wave atomization, 16th Australasian Fluid Mech. Conf., Gold Cost, Australia, 2-7 Dec. 2007.

Anandharamakrishnan C., Computational Fluid Dynamics Applications in Food Processing, Springer, Berlin, 2013.

Astrom K., Wittenmark B. Computer-controlled systems, Prentice Hall, 1996.

Astrom K., Hagglund T. Advanced PID control, ISA, 2005.

Astrom K., Wittenmark B. Adaptive control, Prentice Hall, 1994.

Aydin M., Gunaydinoglu E., Aydin M., Miguel A. Gas-solid suspension flow near walls: Particle statistical mechanics model and particle force balance equation, Defect Diffusion Forum, 348, 71-87, 2014.

Balaji C. Essentials of radiation heat transfer, J. Wiley, Chichester, UK, 2014.

Bjelobrk N., Nabavi M., Poulikakos D., Acoustic levitator for contactless motion and merging of large droplets in air, J. Appl. Phys., 053510, 112,

Bohlin T. Interactive system identification: Prospects and pitfalls. Springer, Berlin 1991.

Brandt E., Suspended by sound, Nature, 413, 474-475, 2001.

BUCHI company literature – spray drying, Flawil,Switzerland.

Buesser B., Pratsinis S. Design of nanomaterials synthesis by aerosol processes, Ann. Rev. Chem. Biomol. Eng., 3, 103-127, 2012.

Camacho E., Bordons C., Model predictive control in the process industry, Springer, London, 1995.

Carraro T., Heuveline V., Rannacher R. Determination of kinetic parameters in laminar flow reactors: I. Theoretical aspects. In: Jaeger W., Rannacher R. Warnatz J. (Eds) Reactive flows, diffusion and transports, Springer, Berlin, 2007.

Chaker M., Meher-Homji C., Mee T., Inlet fogging of gas turbine engines – part B: Fog droplet sizing analysis, nozzle types, measurement and testing, Paper 2002-GT-30563, Proc. ASME Turbo Expo, June 3-6, 2002, Amsterdam.

Chen J., Wang L., Du B. Modified Internal Model Control for chemical unstable processes with time delay, Proc. 7th World Congress. Intel. Control Automat. Chongqing, 6353-6358, June 25-27, 2008.

Chhabra R., De Kee D. Transport processes in bubbles, drops and particles. Hemisphere, N.Y., 1992.

Clark R. Control system dynamics. Cambridge Univ. Press, Cambridge, 1996.

Cooper D. Cascade vs. feedforward for improved disturbance rejection, ISA Conf., 5-7 Oct., 2004.

Cooper D. Practical process control, e-book; http://www.controlguru.com/pages/table.html, 2007.

Corredor C., Bu D., Both D., Comparison of near infrared and microwave resonance sensors for at-linemoisture determination in powders and tablets, Analyt. Chim. Acta, 696, 84-93, 2011.

Crosby K. et al. Inertial filtration of lunar dust in reduced gravity, 4073, Joint Annual Meeting LEAG-ICEUM-SRR, 2008.

Dalmoro A., d'Amore M., Barba A., Droplet size prediction in the production of drug delivery microsystems by ultrasonic atomization, Transl. Med., 7, 6-11, 2013.

Datta A. Adaptive Internal Model Control, Springer, London, 1998.

Delendik K., Saverchenko V., Fisenko S. Pyrolysis of a femtoliter drop in a low-temperature aerosol reactor at lowered pressure, J. Eng. Phys. Thermophys., 85, 549-553, 2012.

Dombrovsky L., Bailis D. Thermal radiation in disperse systems: an engineering approach, Begell House Inc, 2010.

Drummond C., Chan D., Theoretical Analysis of the Soiling of "Nonstick" Organic Materials, Langmuir, 12, 3356-3359, 1996.

Ebner P., Lipinski W. Heterogeneous thermochemical decomposition of a semi-transparent particle under direct irradiation, Chem Eng Sci, 66, 2677-2689, 2011.

Emerson/Micro Motion, company literature, St. Louis, MO, 2014.

ETHOS Environmental and Thermal Operating Systems, Console Handbook, International Space Station document, 2014.

Ezell M., Chen H., Arquero K., Finlayson-Pitts B. Aerosol fast flow reactor for laboratory studies of new particle formation, J. Aerosol Sci., 78, 30-40, 2014.

Fogmaster, company literature, Deerfield Beach, FL, 2014.

Friauf W. Feedback loop stability analysis, McGraw-Hill, NY, 1998.

Fu N., Woo M., Chen X., Single droplet drying technique to study drying kinetics measurement and particle functionality, Drying Technol..30, 1771-1785, 2012.

Fuchs N. The mechanics of aerosols, Dover Publ. NY, 1989.

Fujisaki Electric, Spray Drying company literature, Anan, Tokushima, Japan.

Fujisaki Electric, US Patent US005845846, 1998; authors: Watanabe O., Kawashima K., Nagao K., Mori H.

GEA Niro company literature: Cleaning-in-Place of Spray Drying Plant, Copenhagen, 2012.

GEA Niro company literature, Drynetics, Copenhagen. 2009-2014.

Gharraei R., Esmaeilzadeh E., Baheri S. Evaluation of two-phase turbulence closure models modifications in near wall region of boundary layer, 16 th Australasian Fluid Mech. Conf. Gold Coast, Australia, 2-7 Dec. 2007.

Gianfrancesco A., Turchiuli, C., Dumoulin E. Powder agglomeration during the spray-drying process: measurements of air properties, Dairy Sci. Technol. 88, 53-64, 2008.

Godoy W., DesJardin P. Radiation driven evaporation of polydisperse water sprays, Intl J. Heat Mass Transfer, 52, 2893-2901, 2009.

Grisso R. et al. Nozzles: Selection and sizing, Virginia Tech, Publication 442-032, 2014.

Grosshans H. Evaporation of a droplet, MVK160 Report, Lund University, 2012.

Guha A. Transport and deposition of particles in turbulent and laminar flow, Annu. Rev. Fluid Mech., 40, 311-341, 2008.

Gurav A., Kodas T., Pluym T., Xiong Y. Aerosol processing of materials. Aerosol Sci Technol. 19, 411-452, 1993.

Haber R. Bars R. Predictive Control in Process Engineering, Wiley-VCH, 2011.

Hanf A., Volpp H., Wolfram J. Determination of kinetic parameters in laminar flow reactors. II. Experimental aspects. In: Jaeger W., Rannacher R., Warnatz J. (Eds) Reactive flows, diffusion and transport, Springer, Berlin, 2007.

Hardalupas Y., Sahu S., Taylor A. Experimental characterization of isothermal and evaporative sprays, ILASS 23rd Ann. Conf., Brno, September 2010.

Hausen H. Heat transfer in counterflow, parallel flow and cross flow. McGraw-Hill, N.Y. 1983.

Hsiao T., Chen D., Greenberg P., Street K. Development of a multi-stage axial flow cyclone, aerosol Sci Technol., 44, 253-261, 2010.

Hsiao T., Chen D., Greenberg P., Street K., Effect of geometric configuration on the collection efficiency of axial flow cyclones, J. Aerosol Sci., 42, 78-86, 2011.

Huang H. et al. Experimentation with aerosol bonsetan, pirfenidone, treprostinil and sidenafil, J Thorac Dis. ;6(10):1411-1419, 2014.

Hwang T., Lin J. Combined convection and radiation heat transfer to thermally developing laminar droplet flow in concentric annuli, Warme- und Stoffubertragung 27, 385-391, 1992.

Ikeuchi Co. Ltd, spray nozzles literature, Osaka, Japan.

Inamura I., Shirota M., Tsushima M., Kato M., Hamajima S., Sato A., Spray characteristics of prefilming type of airblast atomizer, ICLASS 2012, 12th Intl Conf. Liquid Atomiz. Spray Syst., Heildelberg, Germany Sept. 2-6, 2012.

Incropera F., DeWitt D. Fundamentals of heat and mass transfer. J. Wiley, N.Y. 1996.

Isidori A., Marconi L., Serrani A. Robust Autonomous Guidance – An Internal Model Approach, Springer, London, 2003.

Julkland W., Golman B. Analysis of slurry drying in a spray dryer, Intl. J. Eng. Technol., 5, 5178-5189, 2014.

Jorgensen F., Lambert P., Accurate Biopharmaceutical Dispensing: Peristaltic or Piston Pumps, Innovations in Pharmaceutical Technology, 78-80, August, 2008.

Kajiyama T., Park K. Influence of air parameters on spray drying energy consumption, Rev. Bras. Prod. Agro, 12, 45-54, 2010.

Kalani A., Christofides P. Modeling and control of titania aerosol reactor, Aerosol SciTechnol, 32, 369-391, 2000.

Keesman K. System Identification, Springer, London, 2011.

Keison Intl, LabPlant spray dryers literature, Chelmsford, Essex, UK.

Kemp I. et al. Experimental study of spray drying and atomization with a two-fluid nozzle to produce fine particles, Eur. Drying Conf. – EuroDrying 2011, Palma de Mallorca, Spain, 26-28 October, 2011.

Keshani S. et al. Spray drying: An overview on wall deposition, process and modeling, J. Food Eng., 146, 152-162, 2015.

Khalizov A., Earle M., Johnson W., Stubley G., Sloan J., Development and characterization of a laminar aerosol flow tube, Rev. Sci. Instrum. 77, 033102, 2006a.

Khalizov A., Earle M., Johnson W., Stubley G., Sloan J. Modeling of flow dynamics in laminar aerosol flow tubes, J. Aerosol Sci. 37, 1174-1187, 2006b.

Kirk Process Solutions Ltd, company literature, Walton-on-Thames, Surrey, UK.

Kontin S et al. Heat and Mass Transfer Accompanied by Crystallization of Single Particles Containing Urea-water Solution, ILASS – Europe 2010, 23rd Ann Conf., Brno, Czech Rep., Sept 2010.

Kramer A. et al., Surface tension measurement for optimization of flotation control, Procedia Eng., 46, 111-118, 2012.

Kurnick S. et al., Attenuation of infrared radiation by fogs. J. Opt Soc Amer., 50(6), 578-583, 1960.

Lahde A, Raula J, Kauppinen E, Production of L-Leucine Nanoparticles under Various Conditions Using an Aerosol Flow Reactor Method, J. Nanomaterials, v. 2008, Article ID 680897.

Landau I. Robust digital control of systems with time delay (the Smith predictor revisited), Intl J. Control, 62, 325-347, 1995.

Lee T., Wang Q., Tan K., Robust Smith-Predictor controller for uncertain delay systems, AIChE J., 42, 1033-1040, 1996.

Li H., Seville P. Effects of excipient formulation on the morphology and aqueous re-dispersibility of dry-powder silica nanoaggregates, Respiratory Drug Delivery, 375‐378, 2008.

Liu T., Wang Q., Huang H., A tutorial review on process identification from step or relay feedback test, J. Proc. Control, 23, 1597-1623, 2013.

Ljung L. System identification, Prentice Hall, 1999.

Luyben W. Process modeling, simulation and control for chemical engineers. McGraw-Hill, N.Y. 1996.

Luz P, Pires A, Serra O, A low-cost ultrasonic spray dryer to produce spherical microparticles from polymeric matrices, Quim. Nova, 30, 1744-1746, 2007.

M&H Technologies, Sensadyne Instrument Div, Flagstaff, AZ, 2014.

Malvern Instruments Ltd, company literature, Malvern, UK.

Masters K. Spray Drying Handbook (1991), Longman, Harlow, England, UK.

Masoumi M. et al. Modeling and control of a naphta thermal cracking pilot plant, Ind. Eng. Chem. Res. 45, 3574-3582, 2006.

Mezhericher M., Levy A., Borde I., Modeling of droplet drying in spray chambers using 2D and 3D computational fluid dynamics, Drying Technol., 27, 359-370, 2009.

Mezhericher M. Theoretical Modelling of Spray Drying Processes, Lambert Acad. Publ., Saarbrucken, Germany, 2011.

Mezhericher M. CFD-based Modeling of Transport Phenomena for Engineering Problems, Proc World Congress on Engineering, vol III, WCE 2012, July 4-6, London, UK.

Miliauskas G., Sabanas V. Interacting heat transfer processes in water droplets, Mechanika, 52, 17-28, 2005.

Miliauskas G., Sinkunas S., Norvaisiene K., Sinkunas K., Modelling of combined heat and mass transfer of water droplets in thermal technology equipment, Frontiers Heat Mass Transfer, 3, 1-6, 2012.

Miliauskas G., Sinkunas S., Norvaisiene K., Sinkunas K., Initial water temperature influence on the thermal state of evaporating droplets, Mechanika, 19, 135-142, 2013.

MitrakosD., Jokinieni J., Backman U., Housiadas C. Aerosol flow in a tube furnace reactor of gas-phase synthesized silver nanoparticles, J. Nanopart. Res., 10, 153-161, 2008.

Mizoe T., Ozeki T., Okada H., Application of a four-fluid nozzle spray drier to prepare inhalable Rifampicin-containing mannitol microparticles, AAPS PharmSciTech, 9, 755-761, 2008.

Morcos V. Performance analysis of industrial bag filters to control particulate emissions, Energy 21(1), 9-14, 1996.

Murata Y., Kudo Y., Yonezawa M., Characteristics of dry fog ionizer, J. Phys., Conf. Ser., 142, 012066, 2008.

Neundorfer, Inc., company literature, Willoughby, OH.

Nguyen N. et al. Interfacial tension measurement with an optofluidic sensor, IEEE Sensors J., 7, 692-697, 2007.

Nobrega S. et al. A study of a wire-plate electrostatic precipitator operating in the removal of polydispersed particles, Braz J. ChemEng, 21(02) 275-284, 2004.

Normey-Rico J., Camacho E. Control of dead-time processes, Springer, London, 2007.

Normey-Rico J., Camacho E., Dead-time compensators: A survey, Control Eng. Practice, 16, 407-428, 2008.

Normey-Rico J., Sartori R., Veronesi M., Visioli A. An automatic tuning methodology for a unified dead-time compensator, Control Eng, Practice, 27, 11-22, 2014.

O'Callaghan D., Hogan S., The physical nature of stickiness in the spray drying of dairy products, Dairy Sci. Technol. 93, 331-346, 2013.

Ocampo-Martinez C. Model Predictive Control of Wastewater Systems, Springer, London, 2010.

Okuyama K., Lenggoro W., Preparation of nanoparticles via spray route, Chem. Eng. Sci., 58 537-547, 2003.

Omer K., Ashgriz N. Spray Nozzles, 497-578; In: Ashgriz N. (ed.) Handbook of atomization and sprays, Springer, NY, 2011.

Ortega-Palacios R., Moreno E., Leija Vera A., Validation of a transit time blood flow meter used for coronary bypass surgery, IEE Ann. Intl Conf., Eng. Med. Biol. 178-181, 2010.

Padhan D., Majhi S. Modified Smith predictor and controller for time delay processes, Electronics Lett., 47, No 17, 2011.

Park B., Lee J., Kihm K. Comparative study of twin-fluid atomization using sonic or supersonic gas jets, Atomiz. Sprays, 6, 285-304, 1996.

Petersen L., Poulsen N., Niemann H., Utzen C., Jorgensen J., A grey-box model fro spray drying plants, 10th IFAC Conf., Mumbai, Dec. 18-20, 2013.

Phanphanit P., Cooper D., Ultrasonic atomization of salt water, ILASS Conference, Sept. 8-10, Lake Como, Italy, 2008.

Pin C. et al. Simulation of spray drying on Piper betle Linn extracts using computational fluid dynamics, Intl Food Res. J. 21(3), 1089-1096, 2014.

Pingali K, Rockstraw D, Deng S, Silver Nanoparticles from Ultrasonic Spray Pyrolysis of Aqueous Silver Nitrate, Aerosol Sci. Tech. 39, 1010-1014, 2005.

Pratsinis S. History of manufacture of fine particles in high-temperature aerosol reactors. In: Ensor D. (Ed.) Aerosol Science and Technology, RTI Press, Research Triangle, NC. 475-507, 2011.

Qiang Z., Chang J., Huang C. Electrochemical generation of hydrogen peroxide from dissolved oxygen in acidic solutions, Water Research, 36, 85-94, 2002.

Ranz W., Marshall W., Evaporation from Drops, Part I, Chemical Engineering Progress, 48, 141–146, 1952.

Reuge N., Caussat B., A dimensionless study of the evaporation and drying stages in spray pyrolysis, Comput. Chem. Eng., 31, 1088-1099.

Rogers C., Eaton J. The effect of small particles on fluid turbulence in a flat-plate, turbulent boundary layer in air, Phys. Fluids A 3, 928-937, 1991.

Roser B. Sterile spray drying for stable liquid 21st century pharmaceuticals, Innov. Pharm. Technol., 19, 50-54, 2005.

Rotronic AG, company literature, Basserdorf, Switzerland, 2014.

Ruppel C., Peters F., Effect of upstream installations on the reading of an ultrasonic flowmeter, Flow Meas. Instrum., 15, 167-177, 2004.

Ruzer L., Harley N. Aereosols Handbook, CRC Press, Boca Raton, 2013.

Sadhal S., Ayyaswamy P., Chung J., Transport Phenomena with Drops and Bubbles, Springer NY, 1997.

Saito T. Measurement of Transmissivity of Infrared Radiation through Fog, Scientific Reports of Tohoku University, Series 5, 8, p.53, 1956.

Saleem M., Krammer G., Effect of filtration velocity and dust concentration on cake formation and filter operation in a pilot scale jet pulsed bag filter, J Hazard. Mat., 144, 677-681, 2007.

Saleh S. Prediction of Air Flow, Temperature and Humidity Patterns in a Pilot Plant Spray Dryer, NUCEJ, 13(1), 55-65, 2010.

Sanderson M., Yeung H., Guidelines for the use of ultrasonic non-invasive metering techniques, Flow Meas. Instrument., 13, 125-142.

Sandle T. Hydrogen peroxide vapour sterilization, in: Sterility, Sterilisation and Sterility Assurance for Pharmaceuticals; 129-141, WoodHead Publ., 2013.

Saravanakumar G., Nayak C., Thirunavukkarasu I., Wahidabanu R. Design and analysis of dead-time compensators for self-regulating and non-self regulating processes with dead time using auto-tuning, IEE Intl Conf. Intelligent Adv. Syst., 1036-1041, 2007.

Sartorius Stedim AG, company literature, Goettingen, Germany.

Sazhin S. Advanced models of fuel droplet heating and evaporation, Progr. Energy Combust. Sci., 32, 162-214, 2006.

Schuck P., Mejean S., Dolivet A., Jeantet R., Thermohygrometric sensor: A tool for optimizing the spray drying process, Innov. Food Sci. Emerg. Technol., 6, 45-50, 2005.

Schuck P. et al. Relative humidity of outlet air: the key parameter to optimize moisture content and water activity of dairy powders, Dairy SciTechnol88, 45-52, 2008.

Scilab v. 5.5.1. Open source software package, Scilab Enterprises, Versailles, 2014.

Scilab v.5.5.1. Scilab/Xcos pour l'enseignement des sciences de l'ingenieur, INRIA, Rocquencourt, 2014,

Seborg D., Edgar T., Mellichamp D. Process dynamics and control. J. Wiley, N.Y., 1989.

Seiberling D. Clean-in-Place for biopharmaceutical processes, Informa Healthcare, N.Y., 2008.

Sensirion AG, company literature, Staefa, Switzerland, 2014.

Shafaee M. et al., An investigation on effect of geometrical parameters on spray cone angle and droplet size distribution of a two-fluid atomizer, J. Mech. Sci. Technol., 25, 3047-3052, 2011.

Sher E., Bar-Kohany T., Rashkovan A., Flash-boiling atomization, Progress Energy Combust. Sci, 34, 417-439, 2008.

Sher I., Sher E. Droplet breakup modeling in spraying, 12th ICLASS Conf, Heidelberg, Sept. 2-6, 2012.

Shraiber A. et al. Turbulent flows in gas suspensions, Hemisphere Publ., N.Y., 1990.

Shrivastava M. et a. Modeling oxidation of soot particles within a laminar aerosol flow reactor using computational fluid dynamics, Aerosol Sci. Tech. 43, 1218-1229, 2009.

Siegel R., HowellJ.,Thermal Radiation Heat Transfer, Taylor and Francis-Hemisphere, Washington, 2001.

Smith M., Knox F. Radiation transfer through an artificial fog used in frost prevention, Weather and Climate 7, 12-20, 1987.

Sono-Tek company literature, Milton, NY.

Sourdille P., O'Dwyer A., An outline and further development of Smith predictor based methods for the compensation of processes with time delay, ISSC Conf. , Limerick, July 1-2, 2003.

Sovani S., Sojka P., Lefebvre A. Effervescent atomization, Progress Energy Combust. Sci., 27, 483-521, 2001.

Spacecraft Maximum Allowable Concentrations for Airborne Contaminants (SMACs), NASA, JSC-20584, November 2008.

Spraying Systems, Co. Spray Technology Reference Guide: Understanding Drop Size, Wheaton, IL.

Takarada J. et al. Measurement of liquid viscosity and density using single piezoelectric resonator with two vibration modes, Jap. J. Appl. Phys. 51, 07GB07, 2012.

Tan L., Ibrahim M., Taip F., Empirical model of spray drying of whole milk powder using nozzle atomizer spray dryer, J. Food Agricult. Envir., 8, 247-252, 2010.

Tan L. ,Taip F., Ibrahim M., Kamil R., Empirical modeling and control for spray drying of orange juice powder, 4th Intl Conf Modeling, Simulation and Applied Optimization, Kuala Lumpur, April 19-21, 2011.

Taniere A., Oesterle B., Monnier J. On the behavior of solid particles in a horizontal boundary layer with turbulence and saltation effects, Experiments in Fluids, 23, 463-471, 1997.

Tasdelen U., Ozbay H. On Smith Predictor-based controller design for systems with Integral Action and Time Delay, 9th Asian Control Conf. (ASCC), 23-26 June 2013.

Terekhov V., Pakhomov M., Flow and Heat and Mass Transfer in Laminar and Turbulent Mist Gas-Droplets Stream over a Flat Plate, Springer, Heidelberg, 2014.

Thomas P. How to tune cascade loops, ExperTune User Conf., Austin, TX, April, 2007.

Thybo P., Hovgaard L., Andersen S., Lindelov J. Droplet size measurement for spray dryer scale-up, Pharm. Dev. Technol., 13, 93-104, 2008.

Timedomain CVD Inc., Hayward, California, 2014; http://www.timedomaincvd.com/CVD_Fundamentals/reactors/tube_reactor.html

Tsai C. et al. Pocket-sized ultrasonic nebulizer for inhalation drug delivery, 2013 Joint UFFC, EFTF, PFM Symp. 1190-1192, 978-1-4673-5686-2/13

Tseng C., Viskanta R. Enhancement of water droplet evaporation by radiation absorption, Fire Safety J., 41, 236-247, 2006.

Umqua Research Company, company literature, Bend, OR.

Varghese S., Gangamma S. Evaporation of Water Droplets by Radiation: Effect of Absorbing Inclusions, Aerosol Air Qual. Res., 7, 95-105, 2007.

Vaughan N., Construction and testing of an axial flow cyclone preseparator, J. Aerosol Sci., 19, 295-305, 1988.

Veeramachaneni S., Watkins J. Robust performance design of PID controllers for time delay systems with a Smith Predictor, Amer. Control Conf. 2462-2467, Portland, June 4-6, 2014.

Veronesi M., Performance improvement of Smith Predictor through automatic computation of dead time, Yokogawa Tech. Rep No 35, 25-30, 2003.

Veronesi M., Visioli A. Simultaneous closed loop automatic tuning method for cascade controllers, IET Control Theory Appl., 5, 263-270, 2011.

Veronesi M., Visioli A., Automatic feedforward tuning for PID control loops, Eur. Control Conf. (ECC), Zurich, July 17-19, 2013.

Visioli A., Piazzi A., An automatic tuning method for cascade control systems, Proc. IEEE Intl Conf. Control Appl. 2968-2973, 2006.

Vodencarevic A. Design of PLC-based Smith Predictor for controlling processes with long dead time, IMECS 2010 Conference, March 17-19, Hong Kong, 2010.

Wang Z., Skogestad S., Robust control of time-delay systems using the Smith Predictor, Int. J. Control, 57, 1405-1420, 1993.

Wang S., Langrish T. The use of surface active compounds as additives in spray drying, Drying Technol., 28, 341-348, 2010.

Wasmund E., Saberi S., Coley K. Modeling of an aerosol reactor for optimizing product properties, AIChE J. 53, 6, 1429-1440, 2007.

Wasmund E., Coley K., In situ sampling uncovers the dynamics of particle genesis and growth in an aerosol tube reactor, J. Mater. Sci 44, 2419-2425, 2009.

White R., King D., Combined experimental and simulation (CFD) analysis on performance of a horizontal tube reactor used to produce carbon nanotubes, 7th Intl Conf. CFD Minerals Process Ind., CSIRO, Melbourne, 9-11 Dec. 2009.

Wiklund D., Peluso M.,Quantifying and specifying the dynamic response of flowmeters; Report by Resemont/Emerson company, 2003.

Wisniewski R., Spray drying technology for brine processing; System design and operation; Technology and systems review. Internal Report, NASA Ames Research Center, Moffett Field, November, 2014.

Woo M. et al. Controlling food powder deposition in spray dryers: Wall surface energy manipulation as an alternative, Journal of Food Engineering 94 (2009) 192–198.

Woo M. et al. Role of rheological characteristics in amorphous food particle-wall collisions in spray drying, Powder Technol. 198, 251-257, 2010.

Yamato Scientific Co., spray dryers literature, Tokyo, Japan.

Yao H. et al., Advanced hybrid type ultrasonic flow meter utilizing state-of-the art pulsed Doppler method along with traditional transit time method, 4th Intl Symp. Ultrasonic Doppler Meth. Fluid Mech. Fluid Eng., 89-93, Sapporo, 6-8 Sept., 2004.

Yarin A., Pfaffenlehner M., Tropea C. On the acoustic levitation of droplets, J. Fluid Mech., 356, 65-91, 1998.

Yeo L. et al. Ultrasonic nebulization platforms for pulmonary drug delivery, Expert Opin. Drug Deliv. 7(6) 663-679, 2010.

Yuan C., Shen T., Electrostatic precipitation, in: Wang L. et al. (ed.), Air pollution control engineering, 153-196, Humana Press, Totowa, 2004.

Zaman A., Bergstrom D. Comparative study of near-wall turbulence models for gas-particle flows, 20th Ann Conf CFD Soc. Canada, Canmore, May 9-12, 2012.

Zenkiewicz M. Methods for the calculation of surface free energy of solids, J. Achiev. Materials Manufact. Eng. 24(1), 137-145, 2007.